SUPRAMOLECULAR FUNCTIONALIZATION OF SINGLE-WALLED CARBON

NANOTUBES

A Thesis
Submitted to the Graduate Faculty
of the
North Dakota State University
of Agriculture and Applied Science

By

Baris Yilmaz

In Partial Fulfillment
for the Degree of
MASTER OF SCIENCE

Major Department
Chemistry and Biochemistry

April 2013

Fargo, North Dakota

Title

SUPRAMOLECULAR FUNCTIONALIZATION OF SINGLE-WALLED
CARBON NANOTUBES

By

Baris Yilmaz

The Supervisory Committee certifies that this *disquisition* complies with

North Dakota State University's regulations and meets the accepted standards

for the degree of

MASTER OF SCIENCE

SUPERVISORY COMMITTEE:

Muhammet E. Kose, Ph.D
Chair

Azer Akhmedov, Ph.D

Seth C. Rasmussen, Ph.D

Svetlana Kilina, Ph.D

Approved:

04/23/2013	Gregory R. Cook, Ph.D
Date	Department Chair

ABSTRACT

Single-walled carbon nanotubes (SWNTs) possess extraordinary mechanical strength, thermal and electrical conductivity. These properties make them very attractive in many applications in the fields of nanotechnology, electronics, and optics. However, most of the SWNT syntheses methods result in different types of chiralities, which determine the electronic and optical properties of the sample. Thus, it is important to selectively solubilize and purify carbon nanotubes if one wants to use them in technological applications. Selective separation of SWNTs by chirality has been the research focus of many scientists. Here, a comparative study for the solubility of SWNTs with polyaromatic hydrocarbons and conjugated polymers was conducted. PEGylated corannulene derivative has been shown to disperse more metallic nanotubes than the commonly used sodium dodecyl sulfate dispersant. Phthalimide containing conjugated materials were found to be effective in solubilizing SWNTs. In addition, the structural and mechanistic implications for high solubility power were discussed for all dispersants.

ACKNOWLEDGEMENTS

TABLE OF CONTENTS

LIST OF TABLES

LIST OF FIGURES

LIST OF ABBREVIATIONS

SWNT   Single Walled Carbon Nanotube

DWNT   Double Walled Carbon Nanotube

nm   Nanometer

PEG   Polyethylene Glycol

µm   micrometer

eV   Electron Volt

CoMoCAT   Cobalt and Molybdenum Oxide as Catalyst

AD   Arc Discharge

PLV   Pulsed Laser Vaporization

HiPco   High Pressure Carbon monoxide Disproportionation

VB   Valance Band

CB   Conduction Band

SDS   Sodium Dodecyl Sulfate

DNA   Deoxyribo Nucleic Acid

a.u.   Arbitrary Unit

GPa   Gigapascal

TPa   Terapascal

DGU   Density Gradient Ultra-centrifuge

DomP   1-Docosyloxymethyl-Pyrene

RBM   Radial Breathing Mode

DOC   Deoxycholate

ssDNA   single strand Deoxyribo Nucleic Acid

mM	milimolar
PEGC	Poly Ethylene Glycol Corannulene
rpm	Revolutions per minute
PDI	Poly Dispersity Index
THF	Tetra Hydro Furan
GPC	Gel Permeation Chromatography

CHAPTER 1. INTRODUCTION

1.1.   Research Background

Carbon nanotubes have cylindrical structures and possess sp^2 hybridized carbon atoms. They are also considered as one of the allotropes of carbon. Researchers in the fields of nanoscience and nanotechnology are interested in their remarkable photophysical, mechanical, chemical, and thermal properties [1]. Based on their structural properties, carbon nanotubes can be classified as single-walled carbon nanotubes (SWNTs), double-walled carbon nanotubes (DWNTs), and multi-walled carbon nanotubes (MWNTs) (Figure 1.1).
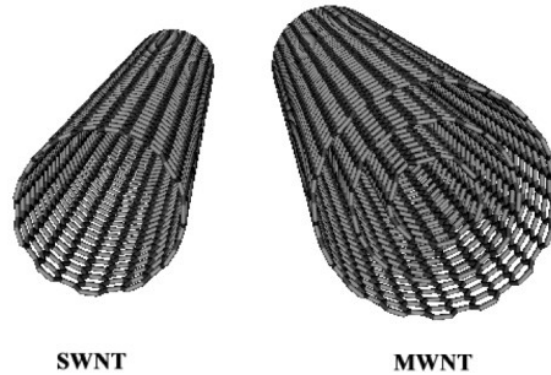
Figure 1.1: Structural features of SWNT and MWNT [1].

The SWNTs' diameters mostly range from 0.36 to 3.37 nm. Using the arc discharge method for the synthesis of SWNTs, the tube length can be tuned between 0.2 and 5 μm [2-5]. The length-to-diameter ratio of SWNTs can reach up to 132,000,000:1, which is the highest aspect ratio for any nanomaterial [5].

MWNTs can have 2-100 nm diameters depending on the number of rolled graphene sheets. The distance between these sheets can be 0.3-0.4 nm, depending on how tightly they are packed in the system. Due to their novel properties, carbon nanotubes can be used in

semiconductor devices [5], nano-probes [6], energy conversion devices [7], sensors [8], field emission displays, and drug delivery systems [9]. However, their high cost, lack of bulk availability, and purification problems hinders their use in aforementioned applications [9].

Since carbon nanotubes are essentially folded version of graphene sheet, they prely consist of sp^2 hybridized carbon atoms within their structure. Therefore, their extended π-electron systems cause highly polarizable surface electrons. As a result, strong inter-tubular van der Waals interactions are present in pristine form of nanotube samples. Almost all production methods lead to carbon nanotube bundles, which are then difficult to separate to individual nanotubes. The typical diameters of bundles can be in the range of a few nanometers to a few microns. The debundling of carbon nanotubes can be achieved with surfactants such as sodium dodecyl sulfate in water, organic aromatic small molecules (anthracene, pyrene) or polymers in organic solvents [9-12]. Covalent side-wall functionalization of nanotubes is also another effective method to improve the solubility in organic solvent or aqueous environment for both SWNTs and MWNTs [13]. Over the years, researchers aimed to find appropriate and unique ways to solubilize the pristine carbon nanotubes for solution processing. Many solvents were tested as a suitable medium for SWNT dispersion with limited success. Some chlorinated solvents were found to be effective in dispersing nanotubes, which have been attributed to relatively strong π-π interaction of solvent molecules with nanotube sidewalls [8-14].

In addition, many techniques were developed during the last decade for selective dispersion of SWNTs. For example, some methods aim dispersion of the carbon nanotubes with planar aromatic hydrocarbons while others employ density gradient centrifuge technique for surfactant solubilized samples [14-20].

1.2. Research Objectives

Although the selective solubility and separation of SWNTs have been reported in the literature by various techniques and dispersants, the bulk separation of SWNTs with cost-effective methods remains a challenge. The structure-property relationships for effective solubilization of nanotubes with dispersant molecules are not known yet.

The main objectives of this thesis are:

(1) To solubilize SWNTs in organic solvents by using non-planar polyaromatic hydrocarbons such as corannulene derivatives for efficient dispersion of SWNTs.

(2) To reveal the structure-property relationships for dispersion capability of conjugated oligomers/polymers in solubilizing carbon nanotube samples.

1.3. Thesis Outline

Chapter 2 gives a brief introduction to structural, electrical and mechanical, and optical characteristics single-walled carbon nanotubes. This chapter also includes various syntheses techniques of SWNTs. The most commonly used nanotube dispersion techniques and relevant dispersant molecules have been discussed in this section.

Chapter 3 provides an outline of characterization techniques for dispersed SWNTs solutions via UV-vis-NIR spectroscopy, resonant Raman spectroscopy, and photoluminescence spectroscopy.

Chapter 4 gives an outline of post-production separation of the single-walled carbon nanotubes via organic materials by using a non-covalent interaction scheme.

Chapter 5 is adapted from "Effective Solubilization of Single-Walled Carbon Nanotubes in THF Using PEGylated Corannulene Dispersant" *ACS Appl. Mater. Interfaces*, 2013, 5 (9), pp

3500–3503. In this chapter, a non-planar corannulene derivative has been exploited in solubilizing SNWTs. The solubilizing power of this new dispersant has been compared to that of well know sodium dodecyl sulfate surfactant. The structural assignments of the debundled individual SWNTs were carried out using the data generated with Raman spectroscopy, 2D excitation-emission spectroscopy and with the help of Kataura plot.

Chapter 6 focuses on the ability of conjugated oligomers/polymers in solubilizing carbon nanotube samples. The structural arrangement of conjugated backbone has important implications in defining solubility power of conjugated materials which are aimed for dispersion studies. This chapter mostly presents preliminary research results obtained with such materials.

Chapter 7 provides a summary, conclusion, and outlook based on this project.

1.4.   References

1.   Akazaki, K.; Toshimitsu, F.; Ozawa, H.; Fujigaya, T.; and Nakashima, N. *Journal of Am. Chm. Soc.*, 2012,**134**, 12700-12707

2.   Ajayan, P.M. *Chemical Reviews*, 1999, **99**, 1787-1799

3.   Lu, F.; Meziani, M. J.; Cao, L.; Sun, Y., *Langimur*, 2010, **27**, 4339-4350

4.   Li, H.; Zhou, B.; Gu, L.; Wang, W.; Fernando, K. A. S.; Kumer, S.; Allard, L. F.; Sun, Y.-P. *J. Am. Chem. Soc*. 2004, **126**, 1014

5.   Wang, W.; Fernando, K. A. S.; Lin, Y.; Meziani, M. J.; Veca, L. M.; Cao, L.; Zhang, P.; Kimani, M. M.; Sun, Y.-P. *J. Am. Chem. Soc*. 2008, **130**, 1415

6.   Liu, C.-H.; Liu, Y.-Y.; Zhang, Y.-H.; Wei, R.-R.; Zhang, H.-L. *Phys. Chem. Chem. Phys*. 2009, **11,** 7257.

7.   Voggu, R.; Rao, K. V.; George, S. J.; Rao, C. N. R. *J. Am. Chem. Soc*. 2010, **132**, 5560

8.   Nish, A.; Hwang, J.-Y.; Doig, J.; Nicholas, R. *J. Nature Nanotechnol*.2007, **2**, 640–646.

9.   Martel, R. *ACS Nano,* 2008, **2**, 2195–2199.

10.   Moore, V. C.; Strano, M. S.; Haroz, E. H.; Hauge, R. H.; Smalley, R. E. *Nano Lett.* 2003, **3**, 1379–1382

11.   Chen, J.; Liu, H.; Weimer, W. A.; Halls, M. D.; Waldeck, D. H.; Walker, G. C. *J. Am. Chem. Soc*. 2002, **124**, 9034–9035.

12.   Tange, M.; Okazaki, T.; Iijima, S. *J. Am. Chem. Soc*. 2011, **133**, 11908-11911

13.   Bonaccorso, F.; Hasan, T.; Tan, T. H.; Sciascia, C.; Privitera, G.; Di Marco, G.; Gucciardi, P., G.; Ferrari, A. C. *J. Phys. Chem. C* 2010, **114**, 17267-17285

14.   Scardaci, V.; Sun, Z.; Wang, F.; Rozhin, A. G.; Hasan, T.; Hennrich, F.; White, I. H.; Milne, W. I.; Ferrari, A. C. *Adv. Mater.* 2008, **20**, 4040.

15.   Bonaccorso, F.; Sun, Z.; Hasan, T.; Ferrari, A. C. *Nature Photon* 2010, **4**, 611

16.   Lee, W.; Chiu, C. S. *Opt. Lett.* 2001, **26**, 521.

17.   Hersam, M. *Nat. Nano.* 2008, **3**, 387.

18.   Krupke, R.; Hennrich, F.; Lohneysen, H. V.; Kappes, M. M. *Science* 2003, **301**, 344.

19.   Egger, R.; Gogolin, A. O. *Phys. Rev. Lett.* 1997, **79**, 5082.

20.   Zheng, M.; Diner, B. A. *J. Am. Chem. Soc.* 2004, **126**, 15490.

CHAPTER 2. SINGLE-WALLED CARBON NANOTUBES

2.1. What is a Single-Walled Carbon Nanotube?

Carbon nanotubes, especially single walled carbon nanotubes, are considered as one of the most promising materials of the 21st century for use in many technological applications. SWNTs were first discovered in 1993 by the scientist working at International Business Machines (IBM) and Nippon Electric Company (NEC) [1]. The structure of SWNT is composed of one-atom thick rolled sheet of graphene [1]. The rolling graphene sheet transforms into a cylinder with various diameters.
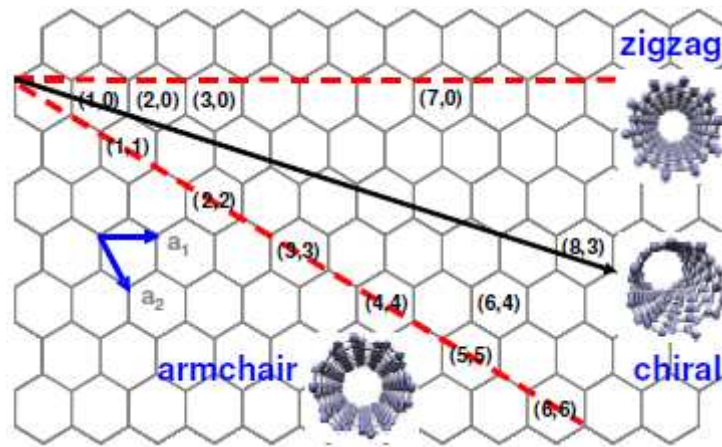
Figure 2.1: Illustration of various types of chiralities
in single-walled carbon nanotubes [2].

The graphene rolling procedure should follow a wrapping angle during the synthesis of SWNTs. Variations in the wrapping angle lead to three different types of nanotubes; zigzag, chiral, and arm-chair. As shown Figure 2.1, the (n,m) nanotube naming scheme stems from the vector sum of two unit vectors in the chiral vector $C_h=na_1+ma_2$. When $n = m$ and the wrapping angle, $\square = 30^o$, forming arm chair SWNTs. In another case when $m = 0$ and $\square = 0^o$, zigzag SWNTs are constructed. Both of these nanotube structures are superimposable on their mirror

image. SWNTs with other wrapping angles ($0^o < \square < 30^o$) are called chiral type carbon nanotubes [3].

Chiral indices (n,m) can be used to calculate both the diameter, d and the chiral angle, $\square$, using the following equations:

$$d = [3(n^2 + m^2 + nm)]^{1/2} b/\pi \qquad (2.1)$$

$$\tan \square = \sqrt{3}m / (2n+m) \qquad (2.2)$$

where b is the distance between two carbon atoms in the flat graphene sheet (for this study 1.44 Å was chosen). Any of these parameters has significant impact on nanotubes' electronic and mechanical properties. Both theoretical calculations and experimental measurements show that when (n-m) mod 3 = 0, the tubes show metallic properties; otherwise tubes present semiconducting properties with energy gap in the order of ~0.5 eV. Thus, pristine nanotube samples have metallic and semiconducting fractions in 1:2 ratio [4].

2.2.   Production Methods of SWNTs

Unique properties of SWNTs allow many potential applications as long as desired amounts of various types of chiralities are sorted selectively and can be processed in solution. Many different techniques (Table 2.1) have been established to produce carbon nanotubes including arc discharge (AD), pulsed laser vaporization (PLV), high pressure carbon monoxide disproportionation (HiPco), and chemical vapor deposition with cobalt and molybdenum oxide as catalyst (CoMoCAT) methods [5].

Table 2.1: Summary of SWNTs Synthesis Techniques and Product Description [6].

Synthesis Methods	Technology of Preparation	Typical mean diameter(nm)	Production Description
Arch Discharge	First reported production	1.5	Less quality, by products, bundled.
Laser Ablation	Ablation from graphite doped with catalyst	1.4	High quality, good diameter control, bundled tubes
Chemical Vapor Deposition	Catalytic chemical vapor deposition, Supported with metal catalyst	1.5	Cheapest, Commercial upscale
Gas phase decomposition	Decomposition oxygen free environment	1.0	Easy to purify, commercial, good quality.

2.2.1. Electric Discharge

The electric discharge method was first reported for producing fullerenes, but it is still one of the widely used techniques for production of SWNTs. Combination of transition metals (Fe, Co, Ni) and rare earth metals (Y and Gd) results in catalytic composite for synthesis of nanotubes [7]. However, the rare earth metals and metal oxides have also been reported as a catalytic medium in this technique. The typical diameter range of produced SWNTs is 0.9-3.1 nm with an average diameter of 1.5 nm [7].

Although this method is not suitable for synthesis of nanotubes with low diameters, it is common and easy to follow, and enables less defects on side walls of nanotubes. This technique also enables large scale production of nanotubes when compared to other methods utilized in this field. However, relatively large amounts of by-products such as graphite, fullerene, multishelled graphite, and amorphous carbon are formed during the production, which amounts to nearly 30% of product weight [7].

2.2.2. Laser Vaporization

The laser vaporization technique is first reported by Smalley's Group in 1995. This technique (Figure 2.2) gives more pure carbon nanotubes than the arc discharge process. It is also possible to produce relatively small diameter carbon nanotubes with an average diameter of 1.4 nm. However, the main disadvantage is the requirement for high purity graphite rods, high laser power, and low production limit in comparison to arc discharge method [8].
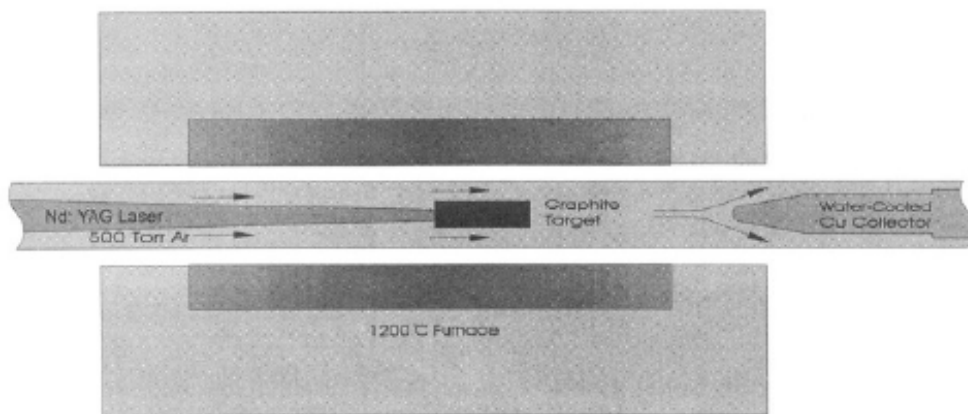
Figure 2.2: Schematic of Laser Vaporization apparatus used at Rice University [8].

2.2.3. Chemical Vapor Deposition (CVD)

Another popular method is the chemical vapor deposition technique. However, the system requires moderate temperatures (700-1473 K) and long reaction times (such as hours). This technique also requires a substrate to grow the carbon nanotubes. Use of substrate, however, allows production of aligned carbon nanotube samples. In addition, many CVD models have been developed to obtain highly pure samples with nanotube diameter of 1 nm up to 2 nm [9].

2.2.4. High Pressure Decomposition of CO (HiPco)

High Pressure Decomposition of CO technique (Figure 2.3) relies on decomposition of continuous-flow carbon monoxide with iron containing carbon monoxide precursor as catalyst.

The production rate is 10 grams/day, and carbon nanotube soot typically contains 5-7 mol % iron (catalytic) impurities. The average diameter of the carbon nanotubes are 1.3-1.4 nm. In comparison to other techniques, this technique allows easy purification of as-synthesized nanotube sample [10].
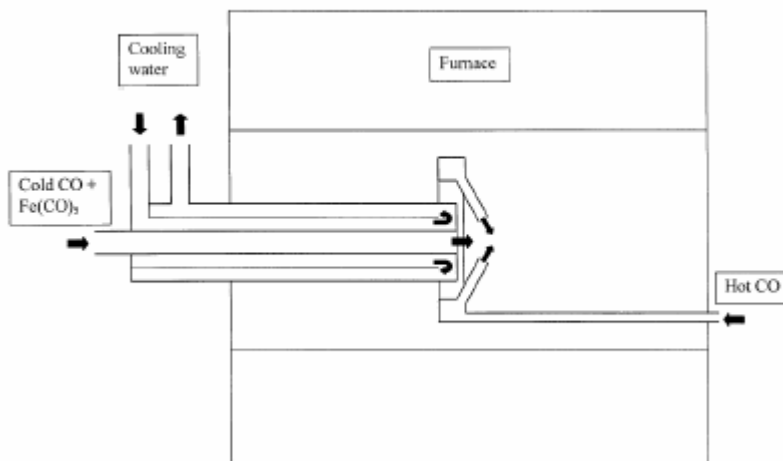
Figure 2.3: Schematic of HiPco processor [10].

2.3.   Electronic Properties of SWNTs

Electronic structure of carbon nanotubes can be determined and explained by band structure of 2-D graphene sheet (Figure 2.4) due to the radial nature of the wave function. On the other hand, the tube chirality might make the VB and CB do not meet at K and K' points and, thus, determine the electronic properties of carbon nanotubes. The electronic structure of the nanotubes is highly dependent on separation of the valence band and conduction band [12]. Carbon nanotubes present metallic properties when these two bands touch each other in K and K' points (Figure 2.5). Electronic properties can also be determined from the chiral index of the carbon nanotube; simply if the chiral index satisfies (n-m) mod 3 = 0, then the nanotube possesses metallic properties. When the K and K' points in the VB are rotated with respect to

those in the CB due to the chiral angle, the difference between n and m are not divided by 3, and the tubes show semiconducting properties. The band gaps of the semiconductor nanotubes vary for various chiralities.

The difference between the electronic structure of graphite and SWNT can be explained in terms of curvative structure affects the non-planar geometry of C-C bonds in SWNTs, the electronic wavefunction quantize the electronic structure to tube axis [14]. In one-dimensional crystals, density-of-states (DOS) is not a continuous function of energy. DOS decreases and then increases in a discontinuous spike. Thus, DOS exhibits a profile with sharp peaks, which are called van Hove singularities. In contrast, such peaks do not exist in three-dimensional materials and those materials have continuous DOS. [11]
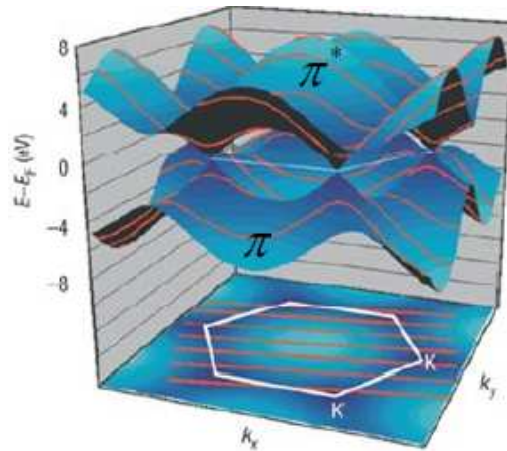
Figure 2.4: Energy band structure of graphene.
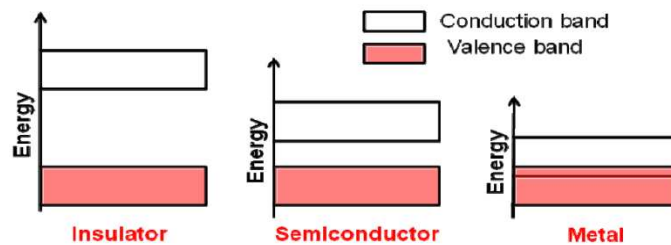
Figure 2.5: Band diagrams of materials [13].

11

2.4.   Optical Properties of SWNTs

SWNTs have a natural ability to form bundles after they are synthesized. The bundles need to be exfoliated to study the optical properties of the individualized carbon nanotubes, because they quench luminescence, presence of metallic tubes in bundles quenches the luminescence from semiconducting tubes due to non-radiative de-excitation. The bundles also lead to inhomogeneous broadening in the absorption spectrum. The photoluminescence spectrum of each nanotube type cannot be determined due to non-radiative relaxation occurring after photo excitation during the presence of metallic carbon nanotubes [15]. Almost a decade later after the first report on carbon nanotubes, sodium dodecyl sulfate (SDS) has been used to disperse SWNTs effectively. O'Connell et al. also reported first photoluminescence spectrum of the individualized nanotubes. The photoluminescence data are evidence for debundling of nanotubes during the sonication process with SDS surfactant [16]. One dimensional density of state is not a continuous function of energy, exhibiting sharp peaks on energy diagram called van Hove singularities. As shown in Figure 2.6, transitions occur among multiple sharp peak locations in between conduction and valence bands. These transitions are named as S_{11}, S_{22}, etc. for semiconducting tubes whereas M_{11}, M_{22} notation is used for transitions in metallic nanotubes [17]. These van Hove singularities provide a unique opportunity to selectively excite individual nanotubes and study their properties. Optical transitions in carbon nanotubes arise from excitonic states. Wang F et al. found out the light absorption produces strongly correlated electron-hole pairs. This finding nullified the previous model where it was claimed that the resonances are as a result of van Hove singularities associated with the one-dimensional structure of the nanotubes. The exciton binding energy of 0.4 eV has been measured for semiconducting nanotubes with 0.8 nm diameter [33]. Excitonic effects have great influence on nanotubes' optical transition energies. The van Hove dominated inter-band transitions are transformed by the inclusion of

excitonic states [34]. The excitonic characters of nanotube's optically excited states, which are similar to the electronic excitations of zero dimensional macromolecular systems, have been modeled with many different theoretical methods. The theoretical predictions reveal exciton binding energies that approach 40% of the tight binding energy band gap. Thus, inclusion of excitonic effects into one-electron band theory model results in better agreement with experiment [35-37].
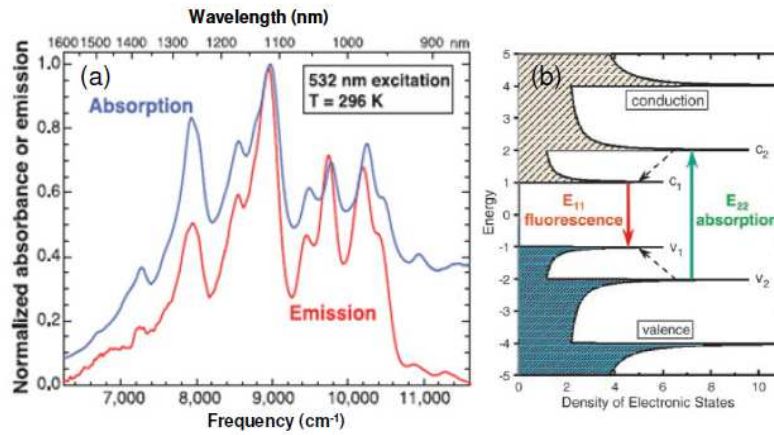
Figure 2.6: (a) Absorption and emission spectra of SWNTs in solution, (b) Schematic diagram of density of states for SWNT [17].

There is a correlation between the nanotube diameter and E_{ii} energies which can be used for prediction of inter band transition energies:

$$E_{ii}^{S,M} = 2\, n\, a_{c\text{-}c}\, \gamma/d \tag{2.3}$$

where $a_{c\text{-}c}$ is the distance between carbon-carbon bonds, γ is the nearest-neighbor C-C interaction energy with constant n. The value of n is 1, 2 and 4 for the first three van Hove transitions in semiconducting tubes and 3 and 6 for the first two van Hove transitions in metallic nanotubes [18-19]. However, the Tight Bonding (TB) model provides only rough estimation for the energies of the experimentally measured optical transitions. Toe get better qualitative picture, TB

13

model has to be extended by using advanced π- band models [29]. These models include next-neighbor hopping overlaps, and site energies for proper modeling of optical spectra of SWTNs [30-32].

2.5. Mechanical Properties of SWNTs

The chemical bonds within single-walled carbon nanotubes are formed by strong sp^2 hybridized orbitals. Each carbon atom is connected to three neighboring carbon atoms, yielding a honey comb lattice. This structural organization gives extra strength on the π-system compared to the stacked graphene sheets. The elastic module of nanotubes is ~1060 GPa. The Young's modulus can reach up to 1 TPa, making these materials very attractive for potential applications [20]. In the study by Anis et al., the mechanical stability of the SWNTs under hydrostatic pressure has been examined. They found pressure induced broadening of the absorbance spectrum of the carbon nanotubes. Even when they apply the lowest pressure onto the sample, the broadened bands blue shifted in comparison to those of the free standing sample [28].

2.6. Methods for Sorting SWNTs

Due to strong van der Waals forces between nanotubes, SWNTs are not soluble in common organic solvents except in a few chlorinated solvents. Thus, great effort has been put forward to develop unique dispersion techniques to separate metallic vs. semiconductor carbon nanotubes, or in general to individually solubilize nanotubes. Many small molecules, oligomers, polymers, surfactants, and bio-macromolecules have been used to produce stable and uniform dispersions. However, most of these dispersants do not show any chiral selectivity; that is all types of chiral nanotubes are present in the final dispersion [21]. Besides, in order to achieve optimal performance from SWNTs in electronic applications, carbon nanotubes should be

dispersed individually with respect to their electronic properties. In this section, post-synthetic approaches are discussed for sorting single-walled carbon nanotubes by chirality [22].

Density gradient ultra-centrifugation (DGU) is one of the most effective techniques to sort the SWNTs by diameter. This technique is generally used for purifying proteins, nucleic acid based materials, and sub-cellular materials. In this technique, density gradient media (generally iodoxanol media) are centrifuged at high speed for a certain time [23]. During the centrifugation process, carbon nanotubes immigrate through from low dense area to high dense area with respect to their isopycnic points. As a result, carbon nanotubes will form layer or layers in the media according to their buoyant density and diameters. With this technique, researchers were also able to separate metallic nanotubes and semiconducting counterparts via the use of co-surfactants as shown in Figure 2.7 [24].
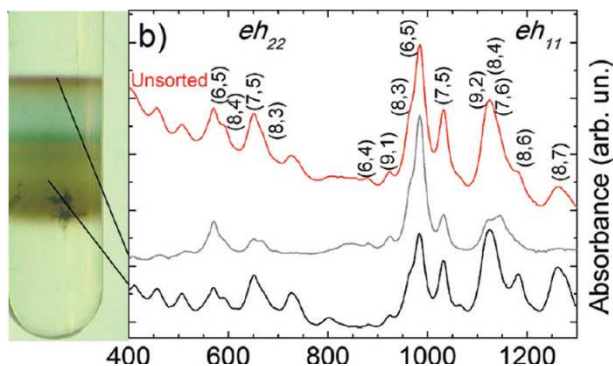
Figure 2.7: Photograph and optical absorbance
spectra of SWNTs after DGU [24].

Ion exchange chromatography technique allows one to separate molecules based on their polarity and ionic charges. This technique has been used for separation of metallic and semiconducting nanotubes, which are wrapped with DNA. Many metallic and semiconductor nanotubes with single chirality were isolated with specific DNA sequences (see Figure 2.8) [25].

As nicely shown in the study performed by Tanaka *et al.*, the semiconductor and metallic carbon nanotubes can also be separated via agarose gel chromatography [26].
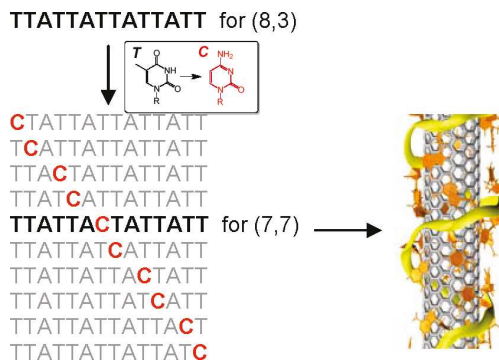
Figure 2.8: A specific DNA sequence
for sorting (7,7) nanotubes [25].

However, very recent studies by Liu *et al*. show that it is possible to obtain single chirality dispersions of SWNTs by a simple gel chromatography, but the method lacks the ability to separate larger diameter tubes, which may be more important for specific applications [26].

Polymers and small molecules and also can also be used for sorting carbon nanotubes via non-covalent interactions. Among these dispersants, coronene, pyrene (Figure 2.9), porphyrin, polyfluorene, and oligocarbazole show good selectivity and dispersion characteristics against SWNTs. More information and relevant details will be given in Chapters 4 and 5 of this thesis.
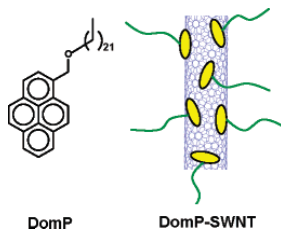
Figure 2.9: Efficient dispersion
of SWNTs can be achieved with
pyrene derivative [27].

2.7. References

1. Bethune, D.S.; Kiang, C.H.; Devries, M.S.; Gorman, G.; Savoy, R.; Vazquez, J.; Beyers, R. *Nature*, 1993, **363**, 605-607.

2. Iijima, S.; Ichihashi, T. *Nature*, 1993, **363**, 603-605.

3. Rao, C.N.R.; Satishkumar, B.C.; Govindaraj, A.; Nath, M. *Chem Phys. Chem*, 2001, **2**, 78-105.

4. Odom, T.W.; Huang, J.L.; Kim, P.; Lieber, C.M., *Nature*, 1998,**391**, 62-64.

5. Wildoer, J.W.G.; Venema, L.C.; Rinzler, A.G.; Smalley, R.E.; Dekker, C. *Nature*, 1998, **391**, 59-62.

6. Tang, Z.K.; Sun, H.D.; Wang, J.; Chen, J.; Li, G.. App. Phys. Let., 1998, **73**, 2287-2289.

7. Nikolaev, P.; Bronikowski, M.J.; Bradley, R.K.; Rohmund, F.; Colbert, D.T.; Smith, K.A.; Smalley, R.E.. *Chem. Phys. Lett.*, 1999, **313**, 91-97.

8. Guo, T.; Nikolaev, P.; Rinzler, A.G.; Tomanek, D.; Colbert, D.T.; Smalley, R.E.. *J. of Phys Chem.*,1995, **99**, 10694-10697.

9. Amama, P.B.; Maschmann, M.R.; Fisher, T.S.; Sands, T.D. *J. of Phys. Chem. B*, 2006, **110**, 10636-10644.

10. Nikolaev, P.; Bronikowski, M.J.; Bradley, R.K.; Rohmund, F.; Colbert, D.T.; Smith, K.A.; Smalley, R.E.. *Chem. Phys. Lett.*, 1999, **313**, 91-97.

11. Kataura, H.; Kumazawa, Y.; Maniwa, Y.; Umezu, I.; Suzuki, S.; Ohtsuka, Y.; Achiba, Y. *Syn. Met.*, 1999, **103**, 2555-2558.

12. Ando, T.*NPG Asia Mat.*, 2009, **1**, 17-21.

13. Javey, A.; Shim, M.; Dai, H.J. *App. Phys. Lett.*, 2002,**80**, 1064-1066.

14. Zhou, C.W.; Kong, J.; Dai, H.J.. *Phys. Rev. Lett.*, 2000, **84**, 5604-5607.

15.   Hartschuh, J., Pedrosa, H., Novotny, L. *Science*, 2003, **301**, 1354

16.   Kataura, H.; Kumazawa, Y.; Maniwa, Y.; Umezu, I.; Suzuki, S.; Ohtsuka, Y.; Achiba, Y. *Syn. Met.*, 1999, **103**, 2555-2558.

17.   O'Connell, M., Bachilo, S., Huffman, C.; *Science*, 2002, **297**, 593

18.   Gao, G.H.; Cagin, T.; Goddard, W.A. *Nanotechnology*, 1998, **9**, 184-191.

19.   Saito, R.; Fujita, M.; Dresselhaus, G.; Dresselhaus, M.S, *App. Phys. Lett.*, 1992, **60**, 2204-2206.

20.   Tibbetts, G. G.; *J.Cryst. Gro.*, 1983, **66**, 347-351

21.   Wang, F.; Itkis, M. E.; Haddon, R. C. *Nano Lett*. 2010, **10**, 937-942

22.   Lu, F., Meziani, J. M., Cao, L., Sun, Y., *Langimur*, 2011, **27**, 4339-4350

23.   Bower, C.; Kleinhammes, A., *Chem. Phys. Lett*., 1998, **228**, 481-486

24.   Bonaccorso, F.; Hasan, T.; Tan, T. H.; Sciascia, C.; Privitera, G.; Di Marco, G.; Gucciardi, P., G.; Ferrari, A. C. *J. Phys. Chem. C* 2010, **114**, 17267-17285

25.   Tu, W.; Walker, A; Khripin, C.; Zheng, M. *J. Am. Chem. Soc*. 2011, **133**, 12998–13001

26.   Kymakis, E.; Klapsis, G.; Koudoumas, E.; Stratakis, E.; Kornilios, N.; Vidakis, N.; Franghiadakis, Y. *Eur. Phys. J.: Appl. Phys.* 2007, **36,** 257-259.

27.   Li, H.; Zhou, B.; Lin, Y.; Gu, L.; Wang, W.; Fernando, K. A. S.; Kumar, S.; Allard, L. F.; Sun, Y.-P. *J. Am. Chem. Soc.* 2004, **126**, 1014-1015.

28.   Anis, B.; Haubner, K., Bornert, F., Dunsch, L., Rummeli, H., Kuntscher, A. , Phys. Rev. B, 2012, **86**, 155454-5

29.   Correa J. *Phys.: Condens. Matter*,2010, **22**, 275503

30.   Cao J X, Yan X H, Ding J W and Wang D L 2001 J. *Phys.:Condens. Matter* 13 L271

31.   Popov V N and Henrard L 2004 Phys. Rev. B 70 115407

32.   Reich S., Thomsen C. and Ordej P.; 2002 *Phys. Rev. B* **65** 155411, Miyake T and Saito S 200 *Phys. Rev. B* 68 155424

33.   Wang F., Dukovic F., Brus L., Heinz., *Science*, 2002, **308**,838-841

34.   Reich S, Dworzak M., Hofgmann A., ThomsenC., Strano S., *Phys. Rev. B*, 2005, **71**, 033402/1-033402/4

35.   Jones M., Ebgtrakul C., Metzger W., Ellingson R., Nozik A., Heben M., Rumbles G., *Phys. Rev. B*, **71**, 115426/1-115426/9

36.   Pedersen G., T., *Phys. Rev. B*, 2003, 67, 207401/1-207401/4

37.   Mazumdar S., Zhao H., *Phys. Rev. B,* 2004, **93**, 157402/1-157402/4

CHAPTER 3. EXPERIMENTAL TECHNIQUES FOR CHARACTERIZATION OF SWNTS

3.1. UV-Vis-NIR Spectroscopy

3.1.1. Absorption

Light absorption occurs when an electron at ground state is excited to a higher energy level with incident radiation. Figure 3.1 shows a simple schematic based on Jablonski diagram, illustrating absorption, fluorescence, and other photoinduced processes in a molecule after photoexcitation. The frequency of the absorption depends on electronic structure of the material. An optical spectrophotometer can record the wavelengths where incident light is absorbed by the material. Spectral absorbance (A) at a specific wavelength is described by Beer-Lambert Law [1].

$$A = - log \ (\ I \ / \ I_o)$$

(3.1)

where I_o and I are the incident light intensity and transmitted light intensity, respectively.

The absorbance of the sample is related to the molar concentration (c) and sample pathway (l) via molar extinction coefficient ε.

$$A = \varepsilon \ x \ c \ x \ l$$

(3.2)
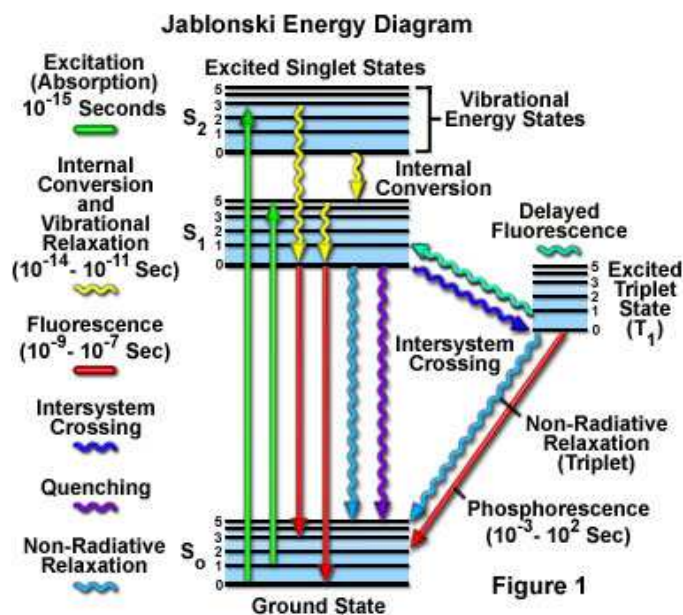
Figure 3.1: Jablonski energy diagram [1].

3.1.2. UV-Vis-NIR Spectroscopy of SWNTs

One of the most important characterization techniques for SWNTs is UV-Vis-NIR spectroscopy, which is an analytical method ideal for determining the magnitude and energy levels of inter-band electronic transitions. These electronic transitions present a unique way to characterize chiralities of SWNTs [2]. In addition, optical absorption spectroscopy is useful in determining the individualized nature of dispersed nanotubes [3]. Figure 3.2 shows typical optical absorption spectra of SWNTs prepared with SDS surfactant. The absorbance between 350 nm to 550 nm is due to presence of metallic nanotubes and called M_{11} region. Other regions in the spectra belong to semiconducting nanotubes [4]. The presence of many types of chiralities makes the optical spectrum difficult to analyze. Sometimes bundles and impurities also contribute to the spectra, which further complicate the analysis [6].

21
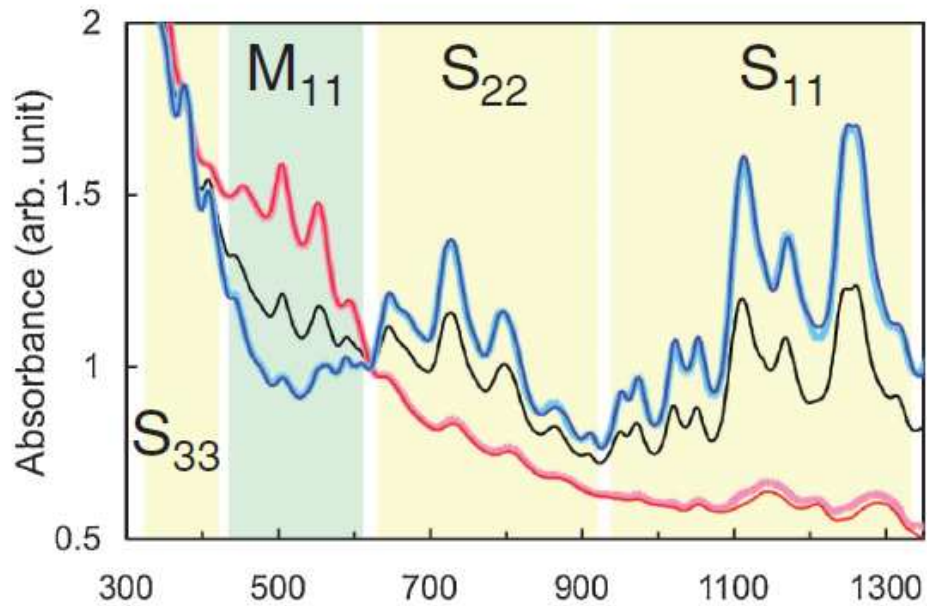
Figure 3.2: Optical spectra of HiPco SWNTs dispersions with SDS [5].

3.2.   Resonant Raman Spectroscopy

Resonant Raman Spectroscopy is one of the most important characterization techniques used for carbon nanotubes. One can obtain information qualitative and quantitative information of diameter, relative abundance, purity, and chirality. Yet, this technique requires very little amount of sample. When the laser light interacts with the sample, electrons make transitions to higher energy levels by interacting with the phonons before transitioning back to ground state [7]. Laser energy does not affect the Raman shift, but when laser energy is resonant to electronic transition, then the Raman intensity of phonon modes increases due to resonance enhancement. Raman scattering, thus, gives information about vibrational modes of nanotubes at the excitation energy of the laser. Horiba Jobin Yvon Aramis Confocal Raman Imaging System spectrophotometer is used in our studies. The instrument laser lines are at 532 nm and 785 nm to determine semiconducting and metallic species separately [8].

3.2.1. Raman Spectroscopy of SWNTs

The typical Raman spectrum of a SWNT sample shows Raman active modes such as radial-breathing modes, (RBMs), D-band (disorder), G-band, and other second-order scattering peaks (Figure 3.3). The RBM occurs due to isotropic radial expansion of the carbon nanotube which presents a unique signature for each nanotube type [9].
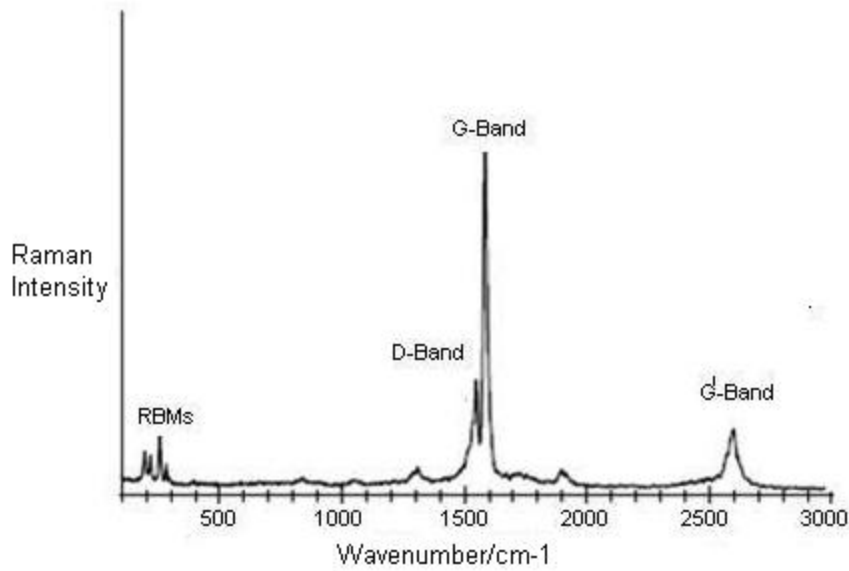
Figure 3.3: Raman spectrum of HiPco SWNTs obtained by using a laser excitation wavelength of 633 nm. Adapted from R. Graupner, J. Raman Spec., 2007, 38, 673.

3.2.1.1. The Radial Breathing Mode (RBM)

The radial breathing mode is the phonon mode that corresponds to radial expansion and contraction of nanotube, as shown in Figure 3.4. RBM frequencies typically show up at lower frequencies, between ~75-350 cm^{-1} in Raman spectra. The radial breathing mode frequency is related to the diameter of the tube with the following formula;

$$\omega_{RBM} = A/d + B \tag{3.3}$$

where A and B are constants [10].
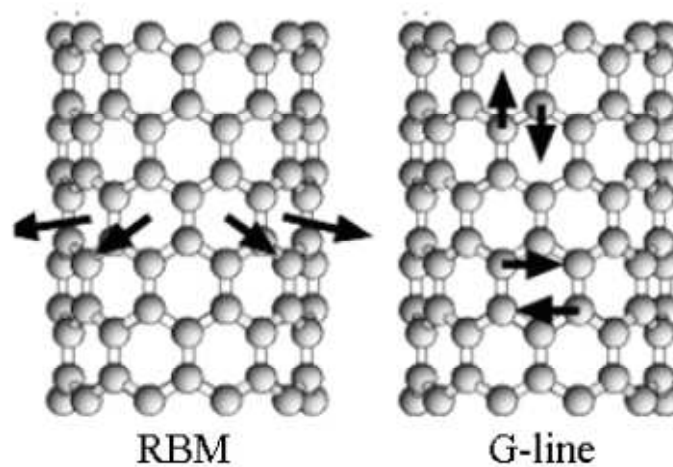
Figure 3.4: The RBM and G modes of a nanotube.

Because of their dependence on tube diameter, the RBM modes are largely used for characterization of the diameter and chiral indices of nanotube samples at the laser excitation line. The radial-breathing frequencies have become the most important feature for determining nanotube chiralities [11].

The Kataura plot, shown in Figure 3.5, is very useful for determining tube diameters and chiralities. Each laser frequency is in resonance with specific radial-breathing modes. When the laser energy is close enough to E_{ii}, the tube gives a strong Raman RBM signal. In order to fully characterize a sample, many different laser sources should be employed [13]. The tube bundling affects the width of RBMs. The individually solubilized nanotubes show narrow, well separated peaks whereas SWNT bundles give broadened RBM peaks [13].
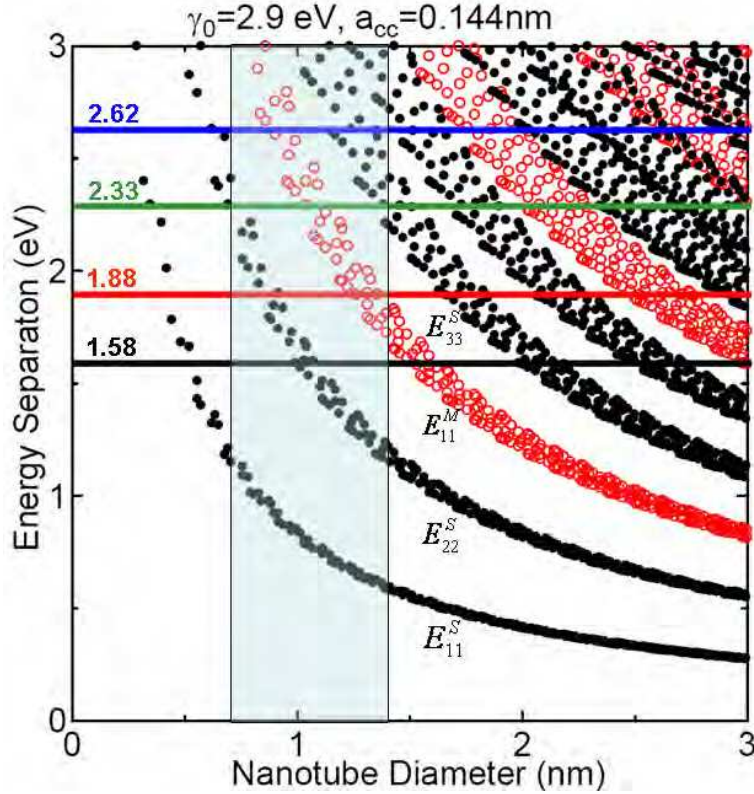
Figure 3.5: In this Kataura Plot, black circles represent semiconducting nanotubes and red circles represent metallic nanotubes [12].

3.2.1.2. The G-band

The graphite-like band (G-band) in carbon nanotubes is related to G-band of graphene. It occurs due to in plane vibrations of carbon atoms. The graphitic G-band is located around ~1582 cm^{-1} at Raman spectrum. However, due to folded graphene sheet G-band splits into two different peaks; the one with lower frequency is called G^- band and the one with higher frequency is called G^+ band. When the metallic carbon nanotubes are abundant in the sample, the G^- band broadens and takes Breit-Wigner-Fano lineshape [14]. However, neither metallic nor semiconducting nanotubes do not show any significant difference in the width and frequency of G^+ band. Breit-Wigner-Fano shaped G^- band is attributed to the presence of metallic carbon nanotubes.

25

However, there is still a controversy regarding the nature and physical explanation of G^- and G^+ bands [15]. Figure 3.6 shows the locations and relative intensity of G^- and G^+ bands when the sample is excited with different laser energies. It is clear that there is an enhancement in G^- band intensity with 2.33 eV excitation. G^+ band dominates at 1.58 eV. That means, mostly metallic nanotubes are in resonance with 1.88 eV excitation whereas 1.58 eV excitation line is mostly in resonance with semiconducting nanotubes [16]. Such information is useful in predicting the relative abundance of metallic and semiconducting nanotubes in an unknown sample.

Figure 3.6: G and D bands at different laser excitation energies [16].

G^+ and G^- bands also related to longitudinal and transverse optical phonons. Fouquet et al found that G^- band is relevant to the metallic carbon nanotube fraction in the sample and G^+ mode is mostly relevant to the semiconducting carbon nanotubes. However, there is still debate
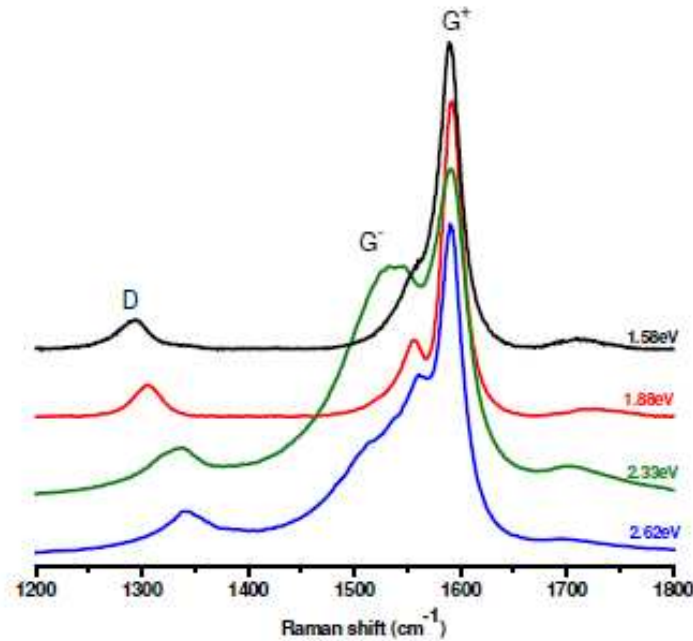
regarding the origin of the G bands and G$^-$ band is usually broad with more features and is highly dependent on the tube diameter [21-22].

3.2.1.3. The D and D* modes

The D band frequency also shows strong dependence on the wavelength of laser energy (Figure 3.6). In addition to D band, it is common to see D* overtone band in the Raman spectrum, which is located at 2500-2900 cm^{-1}. The D band is related to the defects both in the graphite sheets and the carbon nanotubes. The magnitude of D band can be correlated to the amount of defects at end of the tube, amorphous carbon, and any chemical attachments. The relative intensity of D band gives an idea regarding the quality of carbon nanotube sample [17].

3.3.   Photoluminescence Spectroscopy

The photoluminescence spectroscopic studies on SWNTs began after nanotubes were isolated and purified in order to determine the chirality of each semiconducting carbon nanotube species. The absorption spectrum shows a series of sharp peaks once the bundles are removed from the solution. In addition, sharp emission peaks are observed from individualized carbon nanotubes, especially in the near IR region. Only semiconducting nanotubes give photoluminescence, as one might expect [18].

Since there are many nanotubes present in a typical solubilized SWNT sample, it is therefore necessary to collect photoluminescence data at multiple excitation wavelengths. This yields to 2D excitation-emission map. The spectral intensities observed in such a map can roughly give the relative abundance of each nanotube type, assuming they all possess similar molar extinction coefficients. This particular map is especially useful for identification of relatively high diameter semiconductor nanotubes. The chiral index (n,m) can be identified rather easily and that region of map is called the finger print region. Each peak comes from a specific

resonant absorption E_{22}^S with resonant emission collected at a specific E_{11}^S, thus allowing (n,m) determination of nanotube species [19]. Examples of PL maps for SWNTs functionalized by conjugated molecules are given in Figures 5.3 and 6.6-6.8 and further discussed in detail in Chapters 5 and 6.

In essence, this peak identification method is an alternative way to build up the "Kataura Plot". The families of carbon nanotubes have great importance in photoluminescence map; especially (2n+m) families can be recognized fairly easily on 2D excitation-emission map. The photoluminescence maps are qualitatively similar for carbon nanotubes samples prepared with various methods, but detailed analysis can reveal some minor differences. The overall shift of peak locations with various dispersants can be modeled with theoretical calculations [20].

3.4.   References

1.   Gauglitz, G.; Vo-Dinh, T., Handbook of Spectroscopy. 2003, WILEY-VCH.

2.   Tilley, R. J. D., Colour and Optical Properties of Materials: An Exploration of the Relationship Between Light, the Optical Properties of Materials and Colour. 1999, John Wiley & Sons

3.   Nair, N.; Usrey, M.L.; Kim, W.J.; Braatz, R.D.; Strano, M.S.. *Analytical Chemistry* 2006, **78**, 7689-7696.

4.   Freiman S.; Hooker S.; Migler K.; Sivaram, A.. *National Institute of Standard and Technology, Special publication* 2008, 960-19.

5.   Tanaka, T., Urabe, Y., Nishide, D., Kataura, H.; *Applied Physics Express,* 2009, **2**, 125002

6.   Hagen, A., Hertel, T.; *Nano Lett*., 2003, **3**, 383

7.   Long, D.A., The Raman Effect: A Unified Treatment of the Theory of Raman Scattering by Molecules. 2002, *John Wiley & Sons Ltd*.

8.   Thomsen, C.; Reich, S. Raman scattering in carbon nanotubes. Light Scattering in Solids Ix 2007, **108**, 115-235.

9.   Rao, A.M.; Richter, E.; Bandow, S.; Chase, B.; Eklund, P.C.; Williams, K.A.; Fang, S.; Subbaswamy, K.R.; Menon, M.; Thess, A.; Smalley, R.E.;Dresselhaus, G.; Dresselhaus, M.S.. *Science* 1997, **275**, 187-191.

10.   Jorio, A.; Pimenta, M.A.; Souza, A.G.; Saito, R.; Dresselhaus, G.; Dresselhaus, M.S.. *New Journal of Physics* 2003, **5**, 139.

11.   Bachilo, S., Weisman, R., B.,; Nano Lett, 2003, 3, 1235

12.   Kataura, H.; Kumazawa, Y.; Maniwa, Y.; Umezu, I.; Suzuki, S.; Ohtsuka, Y.; Achiba, Y. *Synthetic Metals* 1999, **103**, 2555-2558.

13.   Fantini, C.; Jorio, A.; Souza, M.; Strano, M.S.; Dresselhaus, M.S.; Pimenta, M.A. *Physical Review Letters,* 2004, **93**, 147406

14.   Thomsen, C.; Telg, H.; Maultzsch, J.; Reich, S. *Physica Status Solidi B-Basic Solid State Physics* 2005, **242**, 1802-1806

15.   Fouquet, M.; Telg, H.; Maultzsch, J.; Wu, Y.; Chandra, B.; Hone, J.; Heinz, T.F.; Thomsen, C. *Physical Review Letters* 2009, **102**,075501.

16.   Jorio, A.; Souza, A.G.; Dresselhaus, G.; Dresselhaus, M.S.; Swan, A.K.; Unlu, M.S.; Goldberg, B.B.; Pimenta, M.A.; Hafner, J.H.; Lieber, C.M.;Saito, R. . Physical Review B 2002, **65**, 155412

17.   Osswald, S.; Flahaut, E.; Ye, H.; Gogotsi, Y. *Chemical Physics Letters,* 2005, **402**, 422-427.

18.   Delzeit, L.; McAninch, I.; Cruden, B.A.; Hash, D.; Chen, B.; Han, J.;Meyyappan, M.. *Journal of Applied Physics* 2002, **91**, 6027-6033

19.   Lefebvre, J., Fraser, J. M., Homma, Y.; Appl. Phys. A: Mater. Sci. Proc, 2004, 78, 1107

20.   Kane. C., L., , MeleE. J.; *Solid State Commun*. 2005, **135**, 527.

21.   Fouquet, M.; Telg, H.; Maultzsch, J.; Wu, Y.; Chandra, B.; Hone, J.; Heinz, T.F.; Thomsen, C. *Phy. Rev.Lett.*2009, **102**,075501.

22.   Jorio, A.; Souza, A.G.; Dresselhaus, G.; Dresselhaus, M.S.; Swan, A.K.;Unlu, M.S.; Goldberg, B.B.; Pimenta, M.A.; Hafner, J.H.; Lieber, C.M.; Saito, *R. Phys. Rev. B* 2002, **65**, 155412.

CHAPTER 4. NON-COVALENT FUNCTIONALIZATION OF SINGLE-WALLED CARBON NANOTUBES

4.1.   Post-Production Separation

As produced single-walled carbon nanotubes incorporate 33% metallic and 67% semiconducting nanotubes. This is a problem since either metallic or semiconducting nanotubes are desired for most of the applications. To remedy this issue, novel methodologies are required to separate semiconducting carbon nanotubes from metallic ones, via Van der Waals repulsion, π-π interaction. For example, semiconducting nanotube enriched samples were observed using the CVD method. However, many selective pre-production methods were not successful in achieving quantitative yield for separation of either fraction. Thus, post-production separation methods are vital to overcome this problem [1].

Tetra-substituted free-base porphyrin is selective toward semiconducting carbon nanotubes [17]. Another planar aromatic compound, 1-docosyloxymethylpyrene (DomP), has also been found to selectively disperse semiconducting carbon nanotubes [2]. In a study reported by Tanaka et al., single walled carbon nanotubes were dispersed in SDS and then were centrifuged and loaded to agarose gels using Sepharose 2B [3]. Semiconducting and metallic carbon nanotubes were separated within eleven hours when SDS is used as surfactant to separate metallic nanotubes and semiconducting counterparts were separated by using deoxycholate (DOC). Selective destruction of either metallic or semiconducting carbon nanotubes by using electrical current also helped in isolation of metallic fraction [6]. On the other hand, two different selective destruction methods were developed in 2005; hydrocarbonation reaction and laser irradiation technique [4]. Some methods involve heating the sample until to a certain temperature, followed by annealing, and finally cleaning the carbonaceous material with a

plasma source. However, the main problem with this method is destruction of small diameter metallic carbon nanotubes ($d < 1.4$ nm), leaving only semiconducting nanotubes in the sample [5].

As reported by Miyata et al, selective oxidation of semiconducting species by doping hydrogen peroxide as oxidizing agent is possible although it is generally assumed that the metallic nanotubes have higher chemical reactivity than the semiconducting nanotubes due to their higher electronic density. In another study, it has been found that pure diazonium salts such as 4-dodecyloxybenzenediazonium tetrafluoroborate selectively react with metallic carbon nanotubes [6]. Due to the fact that functionalized metallic carbon nanotubes are now soluble in organic solvents, metallic carbon nanotubes can be extracted, leaving insoluble portion as the semiconducting fraction.

Many different dispersants have been used for non-covalent functionalization of SWNTs with small and macromolecules. The post-production separations were achieved by using DNA, anionic surfactants, small molecules (pyrene, corranene, pentacene, and porphyrin), and macromolecules (oligomers, polymers, conjugated polymers) [7].

4.1.1. Wrapping by DNA and Surfactants

Density gradient centrifugation system has become the most important tool for separation and purification of single-walled carbon nanotubes. This technique is generally used for small scale separation and purification of SWNTs. The first use of density gradient centrifugation for separation SWNTs has been reported by Hersam et al. After centrifugation, the carbon nanotubes gave layers with their unique colors in the centrifuge tube, which is then harvested by their diameter, and identified with optical absorption spectroscopy [9].

The wrapped ssDNA presents a negative charge on carbon nanotube surface, which helps to separate SWNTs individually and selectively. Though, the semiconducting and metallic species have different polarizability and require an anionic exchange column chromatography after treatment with ssDNA [8]. After the gel chromatography, the resulting dispersion is mixed with liquid agarose gel. After squeezing the gel, the extracted solution is mainly enriched with metallic carbon nanotubes and the gel itself contains highly concentrated semiconducting nanotubes [10].

With DNA functionalization, carbon nanotube sample can be separated into semiconducting and metallic fractions. However, different DNA sequences separate different chirality semiconducting nanotubes as discovered by Tu et al. Among the DNA library of $\sim 10^{60}$ sequences searched, 20 different short DNA sequence gives chromatographic purification with specific chirality [24].

Sodium dodecyl sulfate (SDS) is one of the most common surfactants used for solubilizing carbon nanotubes in water. However, other surfactants such as deoxycholate, sodium dodecyl benzene sulfonate, and sodium deoxycholate also have good solubilizing power. Sorting SWNTs with SDS presents unique advantages such as employing density gradient centrifuge method, diameter separation, metallic versus semiconductor separation, single chirality enrichment, and length separation [11]. Aqueous dispersions of surfactant encapsulated nanotubes can be ultra-centrifuged in a gradient media. During the centrifugation, the carbon nanotubes move towards the density gradient media and upon reaching the isopycnic point the carbon nanotubes' buoyant density equals density gradient media. The buoyant density depends on the local concentration and pH of the density gradient media. One can achieve the sorting by using the density difference of the surfactant encapsulated nanotubes. It is also possible to

33

separate left handed and right handed carbon nanotubes by encapsulating them with chiral surfactant such as sodium cholate [12].

4.1.2. Wrapping by Small Molecules

Due to their facile synthesis and batch-to-batch reproducubility, small molecules have great potential for separation of metallic or semiconducting SWNTs. As referenced in Fernando et al., the pyrene derivative, 1-docosyloxymethyl-pyrene (DomP), has provided 85% metallic enrichment via non-covalent interactions [13]. In the relevant study, pyrene derivative has been used as doping agent for carbon nanotubes. The enrichment of the sample with metallic carbon nanotubes was confirmed with a combination of absorption and Raman spectroscopy (Figure 4.1). Raman spectrum also shows a Breit-Wigner-Fano feature in the G-band region, much more pronounced than that of the pre-separation of purified sample. However, the mechanism of separation is not clear yet [14]. The coronene tetracarboxylic acid, potassium salt (Figure 4.2) has a large π-skeleton [16]. Heating coronene derivative with a crude nanotube sample resulted in separation of metallic and semiconducting fractions.

The magnitude of S_{11} and S_{22} bands changed with dispersant concentration and temperature of the medium. When 5 mM of coronene derivative is used, the semiconducting nanotubes precipitate out of solution (Figure 4.3). On the other hand, 10 mM of coronene dispersant solution gives a nice separation of metallic species from the crude sample. As a result, concentration of the coronene based dispersant plays an important role in separating nanotubes by chirality.
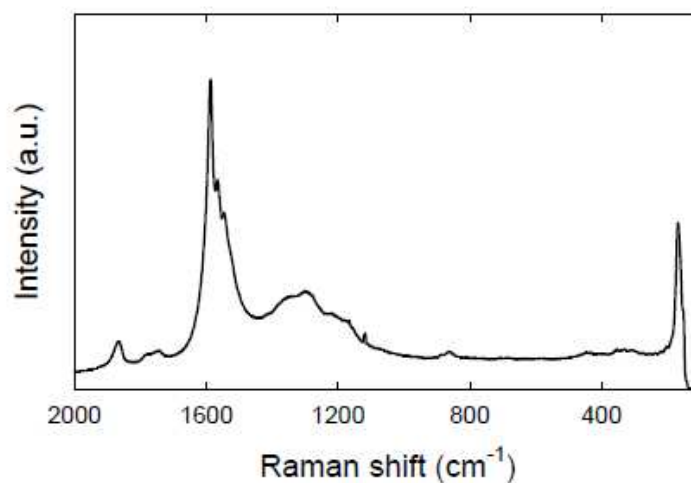
34

Figure 4.1: Raman spectrum (λ_{exc} = 785 nm) of the
DomP-SWNT sample after separation [15].
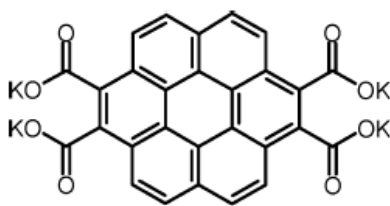
Figure 4.2: Potassium salt of
coronene tetracarboxylic acid.

Raman Spectra also confirm the metallic enrichment with 10 mM of dispersant due to broadening in Breit-Wigner Fano lineshape (Figure 4.4). Another molecule of interest is the free base-porphyrin, which can separate the semiconducting nanotubes from the metallic fraction. When the pristine sample is mixed and sonicated with porphyrin derivative, the dispersant selectively solubilizes the semiconducting nanotubes.
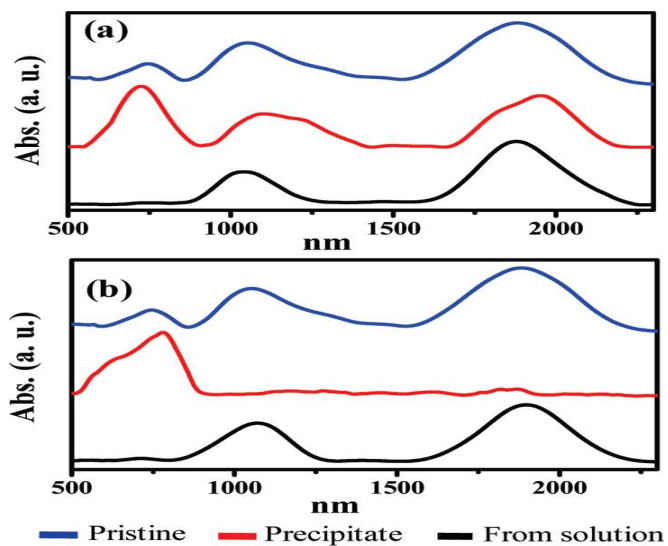
Figure 4.3: Optical absorption spectra of pristine SWNTs (blue), precipitate (red), and SWNTs from solution(black) obtained with (a) 5 mM and (b) 10 mM of coronene derivative.

Figure 4.4: Raman (a) G-band and (b) radial breathing modes (RBM) of sample treated with 10 mM of coronene derivative.

After centrifugation is carried out, the metallic fraction remains as a pellet. With this technique, the individually solubilized SWNT solution can be enriched up to 82% with semiconducting nanotubes (Figure 4.5) [17].

36

Figure 4.5: Schematic of nanotube separation by porphyrin derivative.

4.1.3. Wrapping by Conjugated Polymers

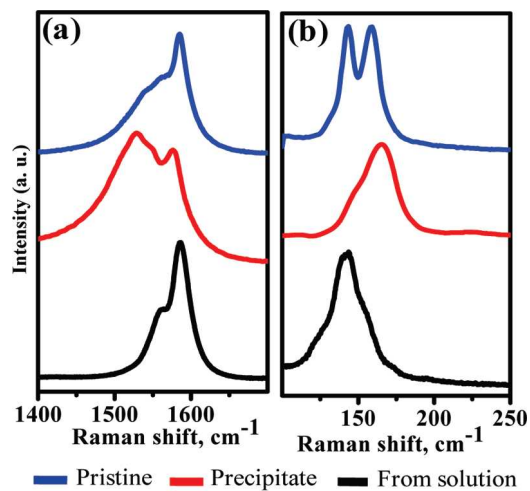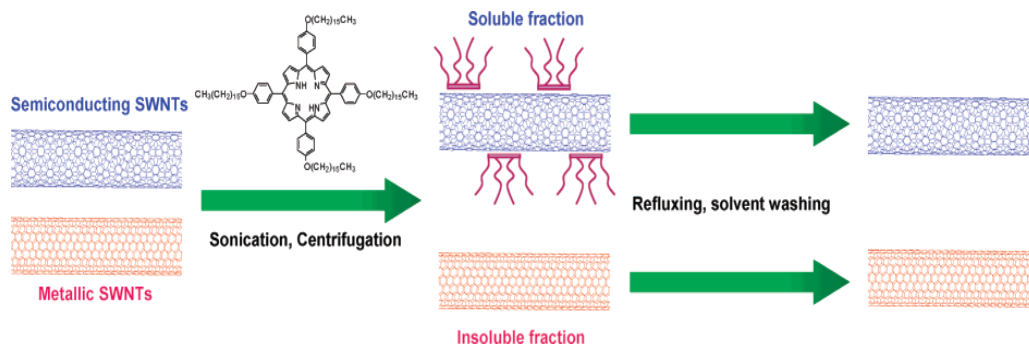Some conjugated polymers such as polyfluorene derivatives show great selectivity toward arm chair nanotubes. Poly(*N*-decyl-2,7-carbazole) is known to disperse mostly semiconducting nanotubes with small chiral angles. This approach is attractive as SWNT separation is possible with a simple technique and low-cost dispersant [19]. Lemasson et al. used density gradient centrifugation method by using 2,4,6-tribromotoluene and toluene mixture as the density gradient media and successfully separated nanotubes by their chiralities. However, they have observed selectivity towards mostly semiconducting nanotubes with the polymers they have used in their study. [20]. In another study of polymer wrapped carbon nanotubes, Tange et al. used poly(9,9-dioctylfluorene-*alt*-benzothiadiazole) to selectively disperse carbon nanotubes with respect to their diameter. Although, the dispersed SWNTs have diameters larger than 1.3 nm, a great selectivity toward (15,4) semiconducting nanotube was obtained in toluene. Within the same study [21], authors claimed the importance of frontier energy level matching of polymers with that of nanotubes for chiral selective dispersion of SWNTs (Figure 4.6). Right or left handed carbon nanotubes can be separated with chiral polymers (Figure 4.7). By changing the ratio of the chiral compound in the polymer structure, researchers were able to collect (6,5) and (7,5) nanotubes in an enriched media [22].
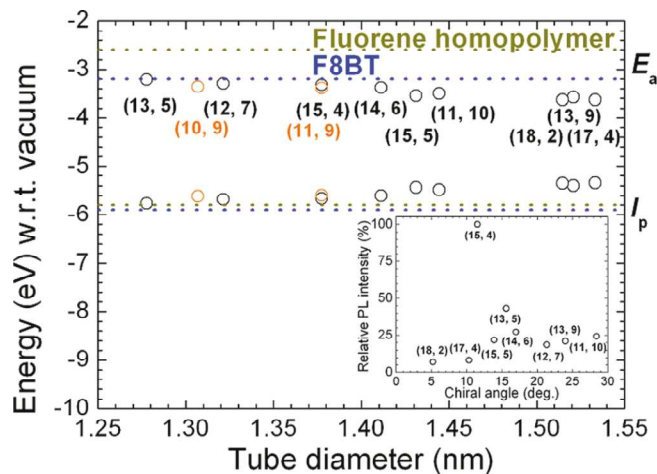
Figure 4.6: Comparison of ionization potentials of
the selected carbon nanotubes with dispersant
conjugated polymers.

In addition, various chiralities were obtained in toluene by modifying the polymer backbone structure. The evidence for enrichment was further confirmed by experiments using UV-Vis-NIR and photoluminescence spectroscopy methods.

Figure 4.7: Schematic drawing of chiral SWNTs and
polymers [22].

4.2.   References

1.   Ajayan, P. M. *Chem. Rev*. 1999, **99**, 1787

2.   Unalan, H. E.; Fanchini, G.; Kanwal, A.; Du Pasquier, A.; Chhowalla, M. *Nano Lett*. 2006, **6**, 677.

3.   Kong, J.; Franklin, N.; Zhou, C.; Chapline, M.; Peng, S.; Cho, K.; Dai, H. *Science* 2000, **287**, 622.

4.   Qu, L.; Du, F.; Dai, L. *Nano Lett*. 2008, **8**, 2682

5.   Arnold,M. S.; Stupp, S. I.; Hersam, M. C. *Nano Lett*. 2005**, 5**, 713.

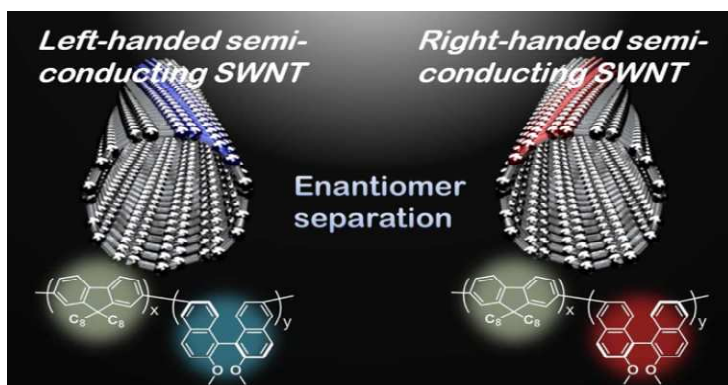6.   Voggu, R.; Govindaraj, A.; Rao, C., N., R., *Ind. J. of Chem*., 2012, 51A, 32-46

7.   Zheng, M.; Jagota, A.; Strano, M. S.; Santos, A. P.; Barone, P.; Chou, S. G.; Diner, B. A.; Dresselhaus, M. S.; McLean, R. S.; Onoa, G. B.;Samsonidze, G. G.; Semke, E. D.; Usrey, M.; Walls, D. J. *Science* 2003, **302**, 1545.

8.   Tanaka, T.; Jin, H.; Miyata, Y.; Fujii, S.; Suga, H.; Naitoh, Y.; Minari, T.; Miyadera, T.; Tsukagoshi, K.; Kataura, H. *Nano Lett*. 2009, **9,** 1497

9.   Chattopadhyay, D.; Galeska, I.; Papadimitrakopoulos, F. *J. Am. Chem. Soc*. 2003, **125**, 3370.

10.   Li, H.; Zhou, B.; Gu, L.; Wang, W.; Fernando, K. A. S.; Kumer, S.; Allard, L. F.; Sun, Y.-P. *J. Am. Chem. Soc*. 2004, **126**, 1014.

11.   Wang, W.; Fernando, K. A. S.; Lin, Y.; Meziani, M. J.; Veca, L. M.; Cao, L.; Zhang, P.; Kimani, M. M.; Sun, Y.-P. *J. Am. Chem. Soc*. 2008, **130**, 1415.

12.   Ju, S.-Y.; Utz, M.; Papadimitrakopoulos, F. *J. Am. Chem. Soc*. 2009, **131**, 6775.

13.   Niyogi, S.; Hamon, M. A.; Hu, H.; Zhao, B.; Bhowmik, P.; Sen, R.; Itkis, M. E.; Haddon, R. C. *Acc. Chem. Res*. 2002, **35**, 1105.

14.   Sun, Y.-P.; Fu, K.; Lin, Y.; Huang, W. *Acc. Chem. Res*. 2002, **35**, 1096.

15.   Basiuk, E. V.; Basiuk, V. A.; Banuelos, J.-G.; Saniger-Blesa, J.-M.; Pokrovskiy, V. A.; Gromovoy, T. Y.; Mischanchuk, A. V.; Mischanchuk,B. G. *J. Phys. Chem. B* 2002, **106**, 1588.

16. Fernando, K. A. S.; Lin, Y.; Wang, W.; Kumar, S.; Zhou, B.; Xie, S.-Y.; Cureton, L. T.; Sun, Y.-P. *J. Am. Chem. Soc.* 2004, **126**, 10234

17. Lu, F.; Wang, W.; Fernando, K. A. S.; Meziani, M. J.; Myers, E.; Sun, Y.-P. *Chem. Phys. Lett*. 2010, **497**, 57.

18. Voggu, R.; Rao, K. V.; George, S. J.; Rao, C. N. R. *J. Am. Chem*. Soc. 2010, **132,** 5560.

19. Pan, X.; Cai, Q. J.; Li, C. M.; Zhang, Q.; Chan-Park, M. B. *Nanotechnology* 2009, **20**, 305601

20. Lu, F.; Wang, X.; Meziani, M. J.; Cao, L.; Tian, L.; Bloodgood, M. A.; Robinson, J.; Sun, Y.-P. *Langmuir* 2010, **26**, 7561.

21. Gu, H.; Swager, T. M. *Adv. Mater.* 2008, **20**, 4433

22. Lu, J.; Lai, L.; Luo, G.; Zhou, J.; Qin, R.; Wang, D.; Wang, L.; Mei, W. N.; Li, G.; Gao, Z.; Nagase, S.; Maeda, Y.; Akasaka, T.; Yu, D. *Small* 2007, **3**, 1566.

23. Akazaki, K., Toshimitsu, F., Ozawa, H., Fujigaya, T.; *J. Am. Chem*. Soc. 2012, **134,** 12700.

24. Tu, X., Manohar, S., Jagota, A., Zheng, M.; *Nat.*2009, **460**, 250-253

CHAPTER 5. EFFECTIVE SOLUBILIZATION OF SWNTs WITH PEGLYATED CORANNULENE DISPERSANT[1]

Adapted from "Effective Solubilizing of Single Walled Carbon Nanotubes in THF Using PEGylated Corrannulene Dispersant" *ACS Appl. Mater. Interfaces*, 2013, 5 (9), pp 3500-3503

Authors: Baris Yilmaz, Josiah Bjorgaard, Christopher Colbert, Jay Siegel, Muhammet E. Köse

5.1. Introduction

In Chapter 4, the capability of a series of aromatic hydrocarbons to disperse and solubilize HiPco SWNTs was evaluated. If SWNTs are dispersed and selected by their chiralities, they can find uses in potential applications such as nano-electronic devices, photovoltaic devices, field-effect transistors, and sensors. SWNTs are 50-100 times stronger than steel [1,2]. In addition, they exhibit anisotropic thermal conductivity that makes them multifunctional materials [3]. However, the pristine form of carbon nanotubes is problematic for large scale applications and fundamental studies due to formation of bundles and occurrence of other carbonaceous materials during the production. The bundles have strong π-π interactions that inhibit their solubility in common organic solvents [4]. SWNTs are wrapped graphene sheets in tubes which are commonly expressed as chiralities (n,m) for different indices [5].

---

[1]The material in this chapter was co-authored by Baris Yilmaz and Josiah Bjorgaard, Christopher Colbert, Jay Siegel, Muhammet E. Köse. Baris Yilmaz had primary responsibility for collecting samples in the field. Baris Yilmaz was the primary developer of the conclusions that are advanced here. Baris Yilmaz also drafted and revised all versions of this chapter. Muhammet E. Köse served as proofreader and checked the graphs which are conducted by Baris Yilmaz.

As-synthesized SWNTs yield a mixture of metallic and semiconducting nanotubes with the metallic component representing the minority fraction in the mixture at a ratio of 1:2, as expected [6,7]. Therefore, the chirality of the SWNT sample defines the electronic and optical properties of nanotubes. As a result, chirality specific SWNTs are needed if these promising materials are to be used in technological applications [8,9].

There are several techniques that have been developed for separation of carbon nanotubes by chirality. Density gradient centrifugation, dielectrophoresis, ssDNA wrapping, and ion exchange chromatography can be used to obtain highly enriched semiconducting or metallic SWNTs up to 90% yield [10,11]. The cost and lack of up-scaling aspects limit the prospect of using such techniques in large-scale applications. Polymer wrapping has also been shown to be effective in chirality and enantiomeric selective separation of nanotubes. Using chiral polymers or porphyrins, one can separate racemic mixtures [12,13].

Non-covalent interactions of nanotubes with polymers or other organic molecules can lead to desired separation of the pristine form. The solubilization has been achieved via planar aromatic molecules (pyrene derivative, free base porphyrin, and coronene) with the possibility of dispersal removal after solubilization [14,15]. In addition, these molecules disperse mostly semiconducting nanotubes without any chiral selectively. Thus, these studies show that there is a great potential for post-production separation of the SWNTs via polycyclic hydrocarbon derivatives [16].

Corannulene is a curved polycyclic aromatic hydrocarbon, consisting of a central cylopentane ring fused with five benzene rings around the core cycle (Figure 5.1). Due to non-planar polyarene structure, it can be considered as a fragment of buckminsterfullerene [17]. The

42

slight bowl shape of corannulene also and extended arene geometry is expected to give better dispersion interactions with respect to similar dispersant used in SWNT solubilization studies [18-23].

Due to loss of planarity, this molecule might give better solubilizing power in comparison to other planar molecules such as pyrene or coronene. In this investigation, short ethylene glycol chains have been attached to the extended arene system to increase the solubility of possible corannulene dispersant-SWNT complex. Ability of this molecule's selective solubilization for specific chiralities has been carefully examined in our studies.
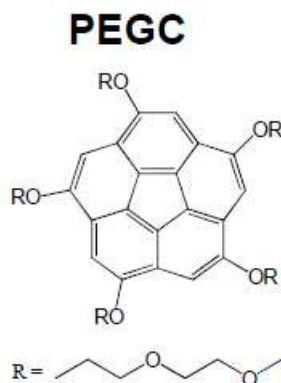

Figure 5.1: Chemical structure of PEGC.

5.2.   Experimental Methods

The corannulene core has been functionalized via attachment of short chains of polyethylene glycol (PEG). PEG groups facilitate solubility both in aqueous and organic solvents. SWNT dispersion with PEGC has been studied using a previously reported method [24]. In a typical experiment 75 mg of PEGC was added into 15 mL of THF and sonicated until PEGC was dissolved completely. After that, 1.6 mg of purified SWNT was added to the solution and then subjected to ultrasonication for 15 min, followed by bath sonication for 3 hrs. The

resulting solution was centrifuged for 45 min at 3000 rpm (Beckman SW40Ti Swing Bucket). The supernatant was carefully transferred to another vial with micro-pipette, producing a dark colored and stable nanotube-dispersant complex solution. The isolated supernatant was filtered through a 200 nm pore diameter Nalgene Teflon membrane and was continuously washed with THF until the filtrate became colorless. Later, 6 mL of THF was added to recover the SWNT residue. The resulting dark solution was further sonicated for 15 min. The solution remains stable for at least 2 months without any observable aggregation and sedimentation.
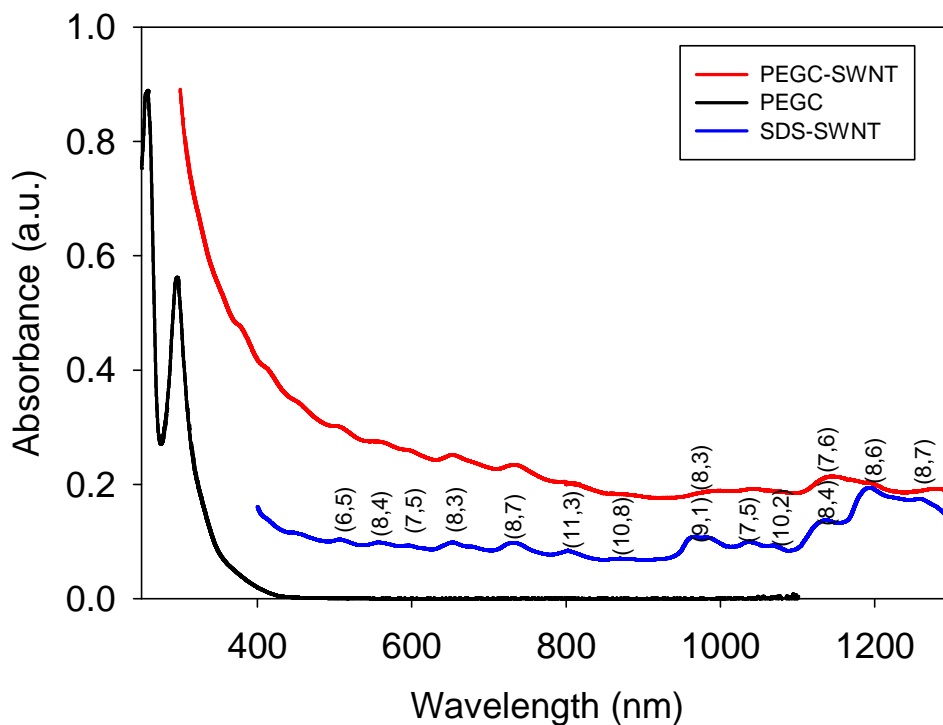

Figure 5.2: Optical absorption spectra of PEGC and PEGC-SWNT in THF. Absorption spectrum of SDS-SWNT sample is also provided for comparison.

5.3. Results and Discussion

The optical absorption of spectrum of PEGC dispersed SWNT solution shows peaks from individually dispersed carbon nanotube species (Figure 5.2). In addition, most of the peaks match

with those of SDS-SWNT dispersed sample. Some major peaks also matched in the 2D excitation-emission maps of both SDS and PEGC dispersed samples, as shown in Figure 5.3. Both maps reveal similar dispersion characteristic exhibited by SDS and PEGC dispersants. The major difference is in the relative amount of specific chiralities solubilized by each dispersant. The resonant Raman modes of SWNT samples were recorded with the laser lines of 532 nm (2.33 eV) and 785 nm (1.58 eV).
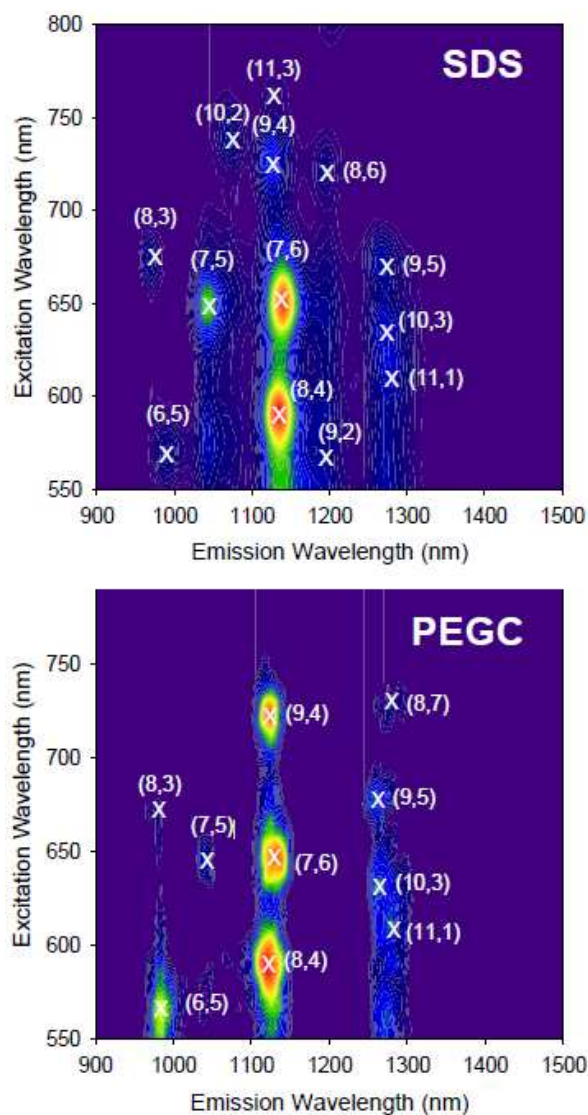

Figure 5.3: 2D excitation-emission maps for samples solubilized by SDS and PEGC dispersants.

Red laser excitation beam is in resonance with Raman active modes of mostly semiconducting carbon nanotubes. The Raman spectra of PEGC-SWNT sample (Figures 5.4-6) show that there is more metallic nanotube species dispersed with PEGC in comparison to the ones dispersed by SDS surfactant. The ratio of the G^-/G^+ is usually taken as a reference to explain the enrichment of metallic species in the dispersed sample. Most of the RBM bands are identified as bands belonging to metallic nanotubes.

Overall, PEGC disperse similar carbon nanotubes as in the SDS dispersion. The ratio of G^- band to G^+ band is 0.14 and 0.10 for PEGC-SWNT and SDS-SWNT samples. Similar measurement on pristine sample is 0.21. As a result, PEGC disperses more metallic carbon nanotubes than SDS. However, the results also suggest –but do not prove- that the metallic/semiconducting ratio does not reach the levels to that of pristine sample for PEGC dispersed carbon nanotube sample.

5.4. Conclusions

We have successfully synthesized (PEGC) a derivative of corannulene. This molecule has showed high solubilizing power for SWNTs. Though, it disperses similar nanotubes as SDS dispersant with little preference to some chiralities. There is, however, a major difference in the amount of dispersion capability against metallic nanotubes when compared to SDS.
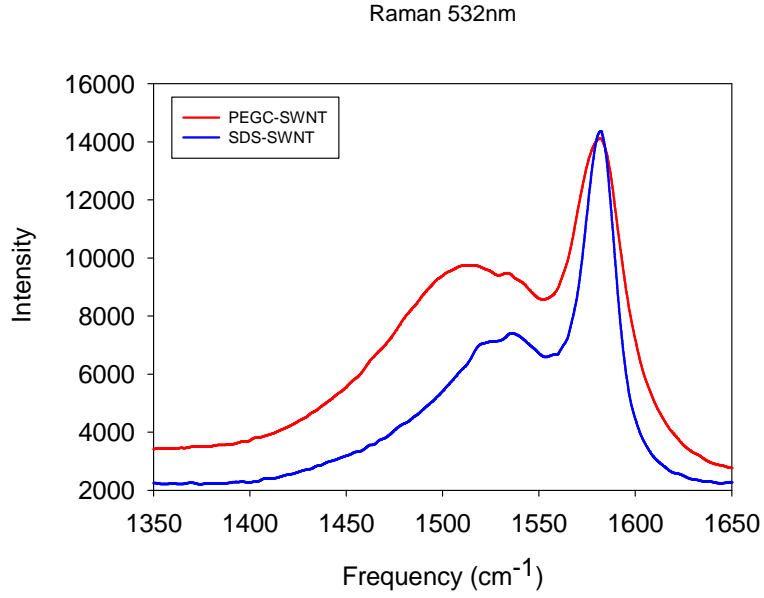
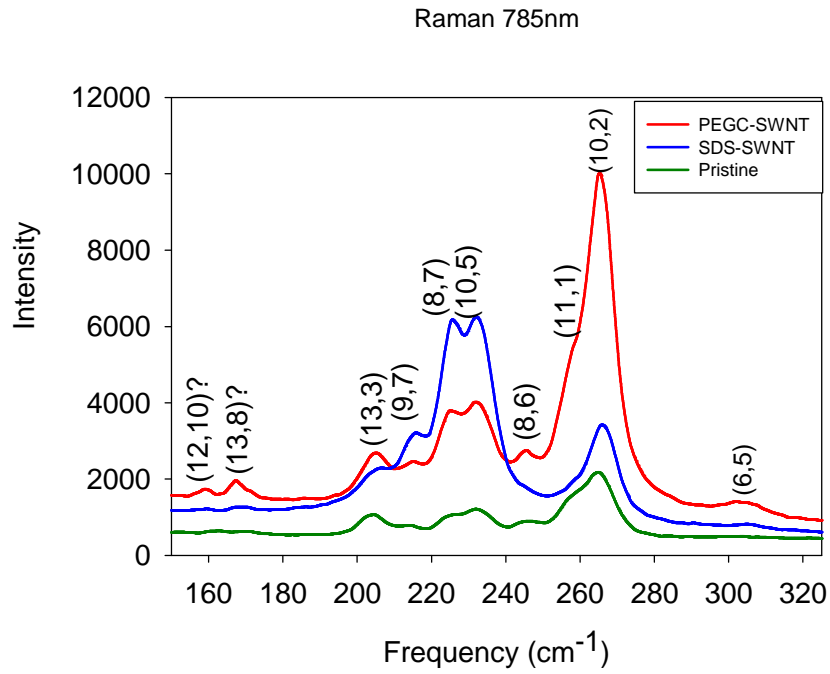Figure 5.4: Solid state Raman spectra of samples excited at 532 nm.

Figure 5.5: Solid state Raman spectra of samples excited at 785 nm.
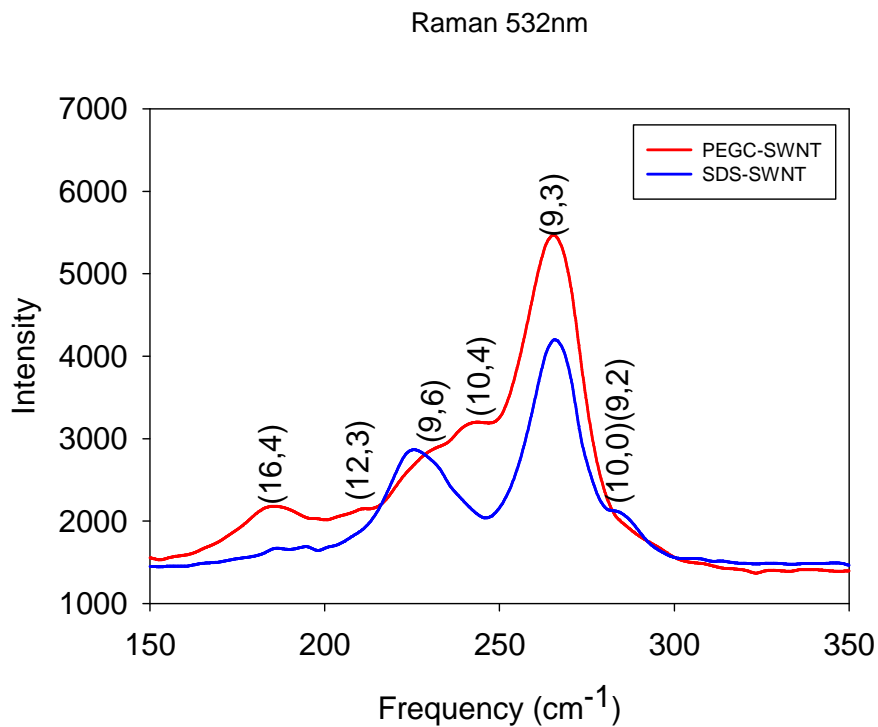
Raman 532nm

Figure 5.6: Solid state Raman spectra of samples for
RBM region excited at 532 nm.

5.5.   References

1.   Ajayan, P. M. *Chem. Rev.* **1999**, *99*, 1787.

2.   Cao, Q.; Kim, H. S.; Pimparkar, N.; Kulkarni, J. P.; Wang, C. J.; Shim, M.; Roy, K.; Alam, M. A.; Rogers, J. A. *Nat.* **2008**, *454*, 495.

3.   Adam, E.; Aguirre, C. M.; Marty, L.; St-Antoine, B. C.; Meunier, F.; Desjardins, P.;Menard, D.; Martel, R. *Nano Lett.* **2008**, *8*, 2351.

4.   Holt, J. M.; Ferguson, A. J.; Kopidakis, N.; Larsen, B. A.; Bult, J.; Rumbles, G.; Blackburn, J. L. *Nano Lett.* **2010**, *10*, 4627.

5.   Hasan, T.; Sun, Z. P.; Wang, F. Q.; Bonaccorso, F.; Tan, P. H.; Rozhin, A. G.; Ferrari, A. C. *Adv.Mat.* **2009**, *21*, 3874.

6.   Itkis, M. E.; Yu, A. P.; Haddon, R. C. *Nano Lett.* **2008**, *8*, 2224.

7.   Kim, S. N.; Rusling, J. F.; Papadimitrakopoulos, F. *Adv.Mat.* **2007**, *19*, 3214.

8.   Krupke, R.; Hennrich, F. *Adv. Eng. Mat.* **2005**, *7*, 111.

9.   Guldi, D. M.; Rahman, G. M. A.; Jux, N.; Tagmatarchis, N.; Prato, M. *Ange. Chem.-Inter.Ed.* **2004**, *43*, 5526.

10.   Arnold, M. S.; Green, A. A.; Hulvat, J. F.; Stupp, S. I.; Hersam, M. C. *Nat. Nanotech.***2006**, *1*, 60.

11.   Krupke, R.; Hennrich, F.; von Lohneysen, H.; Kappes, M. M. *Sci.* **2003**, *301*, 344.

12.   Zheng, M.; Semke, E. D. *J. Am. Chem. Soc.* **2007**, *129*, 6084.

13.   Tu, X. M.; Manohar, S.; Jagota, A.; Zheng, M. *Nat.* **2009**, *460*, 250.

14.   Nish, A.; Hwang, J. Y.; Doig, J.; Nicholas, R. J. *Nat. Nanotech.* **2007**, *2*, 640.

15.   Voggu, R.; Rao, K. V.; George, S. J.; Rao, C. N. R. *J. Am. Chem. Soc.* **2010**, *132*, 5560.

16.   Marquis, R.; Greco, C.; Sadokierska, I.; Lebedkin, S.; Kappes, M. M.; Michel, T.; Alvarez, L.; Sauvajol, J. L.; Meunier, S.; Mioskowski, C. *Nano Lett.* **2008**, *8*, 1830.

17.   Berton, N.; Lemasson, F.; Hennrich, F.; Kappes, M. M.; Mayor, M. *Chem. Comm* **2012**, *48*, 2516.

18.   Wang, F.; Matsuda, K.; Rahman, A.; Peng, X. B.; Kimura, T.; Komatsu, N. *J. Am. Chm. Soc.* **2010**, *132*, 10876.

19.   Li, H. P.; Zhou, B.; Lin, Y.; Gu, L. R.; Wang, W.; Fernando, K. A. S.; Kumar, S.; Allard, L. F.; Sun, Y. P. *J. Am. Chem. Soc* **2004**, *126*, 1014.

20.   Wang, W.; Fernando, K. A. S.; Lin, Y.; Meziani, M. J.; Veca, L. M.; Cao, L.; Zhang, P.; Kimani, M. M.; Sun, Y. P. *J. Am. Chem. Soc* **2008**, *130*, 1415.

21.   Scott, L. T.; Hashemi, M. M.; Meyer, D. T.; Warren, H. B. *J. Am. Chem. Soc* **1991**, *113*, 7082.

22.   Sygula, A.; Fronczek, F. R.; Sygula, R.; Rabideau, P. W.; Olmstead, M. M. *J. Am. Chem. Soc* **2007**, *129*, 3842.

23.   Grube, G. H.; Elliott, E. L.; Steffens, R. J.; Jones, C. S.; Baldridge, K. K.; Siegel, J. S. *Org.Lett.* **2003**, *5*, 713.

24.   Imin, P.; Imit, M.; Adronov, A. *Macromol.* **2011**, *44*, 9138.

CHAPTER 6. SUPRAMOLECULAR FUNCTIONALIZATION OF SINGLE-WALLED CARBON NANOTUBES WITH PHTHALIMIDE CONTAINING OLIGOMERS/POLYMERS

6.1.   Introduction

Fluorene based π-conjugated polymers only disperse semiconducting SWNTs in organic solvents. The rigidity of the conjugated backbone is important for effective π- π interaction with the nanotube surface [1-8]. The polymer wrapping extraction techniques already reported by other groups that are effective for solubilization of low-diameter SWNTs ($d_t < 1.2$ nm). The largest reported tube diameter for extracted semiconducting nanotube is 1.17 nm via poly(9,9-di-octylfluorene) [9-12]. However, methods and dispersants for diameter dependent selective extraction of SWNTs have not been developed yet. The phthalimide containing polymers are particularly interesting due to their good solubility, facile synthesis and processability [13-16].

This class of conjugated polymers is gaining interest in regards to their selective interactions with certain SWNT chiralities [17-20]. Here, we report a full systematical study of the effect of side chains and conjugated backbone structure on dispersion capability of phthalimide containing polymers.

6.2.   Experimental Methods

4,7-bis(5-bromothiophen-2-yl)-2-dodecylisoindoline-1,3-dione [22],9-(2-ethylhexyl)-2,7-bis(4,4,5,5-tetramethyl-1,3,2-dioxaborolan-2-yl)-9H-carbazole [23], (4,4-bis(2-ethylhexyl)-4H-cyclopenta[1,2-*b*:5,4-*b*']dithiophene-2,6-diyl)bis(trimethylstannane) [24], 4,7-dibromo-2-dodecylisoindoline-1,3-dione[25], (3,4'-didodecyl-[2,2'-bithiophene]-5,5'-diyl) bis(trimethylstannane)[26], (3,4'-bis(dodecyloxy)-[2,2'-bithiophene]-5,5'-diyl) bis(trimethylstannane)[27], 4-(5-bromo-3-dodecylthiophen-2-yl)-7-(5-bromo-4-dodecylthiophen-

2-yl)-2-dodecylisoindoline-1,3-dione [28] ,4-(5-bromo-3-(dodecyloxy)thiophen-2-yl)-7-(5-bromo-4-(dodecyloxy)thiophen-2-yl)-2-dodecylisoindoline-1,3-dione [29] were synthesized according to the procedures in the cited literature. Figures 6.1 and 6.2 show the syntheses schemes for polymers and oligomers used in this study. PPC, PPCO, and PPCA were prepared using Suzuki polycondensation reactions from 9-(2-ethylhexyl)-2,7-bis(4,4,5,5-tetramethyl-1,3,2-dioxaborolan-2-yl)-9H-carbazole and corresponding dibromo substituted monomers. The reaction of these monomers were carried out in a mixture of toluene and 2 M Na_2CO_3 solution as the solvent and with $Pd(PPh_3)_4$ as the polymerization catalyst. The reaction yields are higher than 30% in most cases. The crude polymers were purified with soxhlet extraction technique with methanol and acetone as the refluxing solvents. All the polymers have excellent solubility in THF and chlorinated solvents, probably due to presence of bulky side chains.

PPCT, PPTO, and PPTA were prepared using Stille polycondensation reactions with comonomers shown in Figure 6.2. The reactions were carried out in toluene and $Pd(PPh_3)_4$ has been used as the catalyst. Yields and purification steps were similar to those polymers obtained with Suzuki coupling reactions.

[1]H Analysis of Polymers:

PPCT: ^{1}H NMR (CDCl_3, 400 MHz): 8.10 (br, 2H), 6.67 (s, 2H), 3.76 (br, 4H), 2.10 (br,4H), 1.19-1.68(br, 22H), 0.74-0.95 (br, 14H)

PPCO: ^{1}H NMR (CDCl_3, 400 MHz): 8.09 (br, 2H), 7.85 (br, 2H), 7.57 (br, 2H), 7.27 (br, 2H), 4,29 (br, 4H), 4,14 (br,2H) 3.72 (br, 2H), 2.10 (br,4H), 1.19-1.68(br, 32H), 0.74-0.95 (br, 15H)

PPC: ^{1}H NMR (CDCl$_3$, 400 MHz): 8.09 (br, 2H), 7.95 (br, 4H), 7.57-7.35 (br, 4H), 7.27 (br, 2H), 4,29 (br, 4H), 4,17 (br,2H) 3.71 (br, 2H), 2.10 (br,2H), 1.19-1.68(br, 28H), 0.74-0.95 (br, 12H)

PPTA: ^{1}H NMR (CDCl$_3$, 400 MHz): 8.05 (br, 2H), 7.87 (br, 2H), 3.67 (br, 2H), 2.75 (br,4H),1.6-1.8 (br, 6H), 1.19-1.5(br, 54H), 0.74-0.95 (br, 9H)

PPCA: ^{1}H NMR (CDCl$_3$, 400 MHz): 8.10 (br, 2H), 7.87 (br, 4H), 7.55 (br, 2H), 7.47 (br, 2H), 3.72 (br, 4H), 3.275 (br,3H),1.6-1.8 (br, 6H), 1.19-1.5(br, 62H), 0.74-0.95 (br, 12H)

PPTO: ^{1}H NMR (CDCl$_3$, 400 MHz): 8.05 (br, 2H), 7.87 (br, 2H), 4.27 (br, 4H), 3.75 (br,2H),1.6-1.8 (br, 6H), 1.19-1.5(br, 54H), 0.74-0.95 (br, 9H)

The molecular weights were measured using Gel Permeation Chromatography (GPC) with THF as an eluent, with a flow rate of 1 mL/min on a Waters Modular system with 2410 Refractive Index detector and 515 pump. The system utilized a styragel 4E and 5E column and calibrated with polystyrene standards. Molecular weight and polydispersity index (PDI) values of the polymers are listed in Table 6.1. The following recipe has been used for supramolecular functionalization of SWNTs with the conjugated polymers. In a typical experiment, 20 mg of polymer was dissolved in 15 mL of distilled THF. 1 mg of purified SWNT sample (HiPco from Unidym Inc.) was added into the solution and then the mixture was ultrasonicated for 15 min in an ice bath, followed by 3 hours of bath sonication. The resulting solution was centrifuged for 15 min at 5400 rpm using SW 40Ti swing bucket and then supernatant was saved. The dark colored solution was filtered through Nalgene 200 nm Teflon filters and the solid was washed continuously with THF until the entire free polymer fraction is removed. Then, 5 mL of THF was added to recover the residue. The solution was further sonicated for 15 minutes, producing a relatively dark solution, which was then used in spectroscopic measurements.
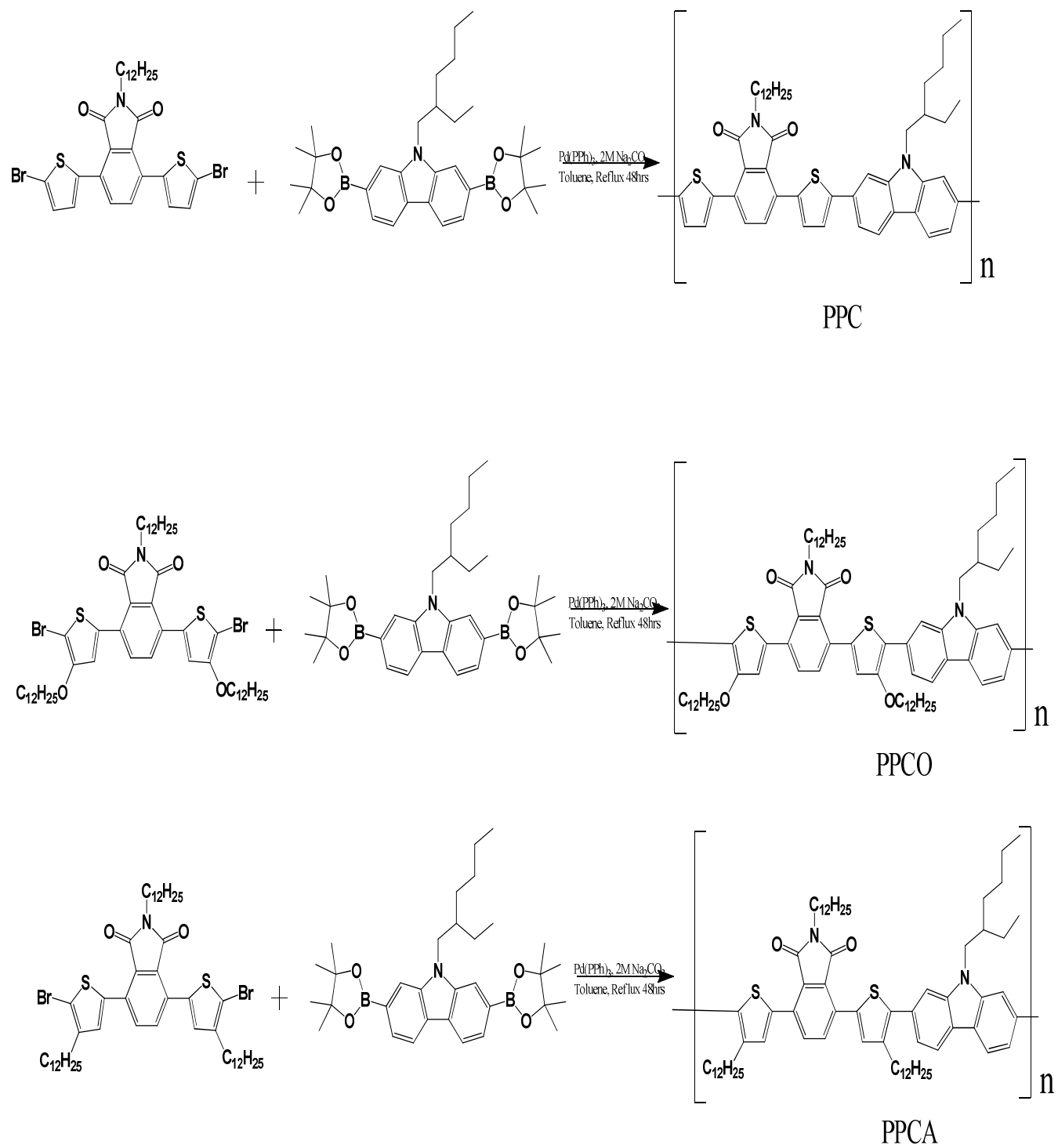
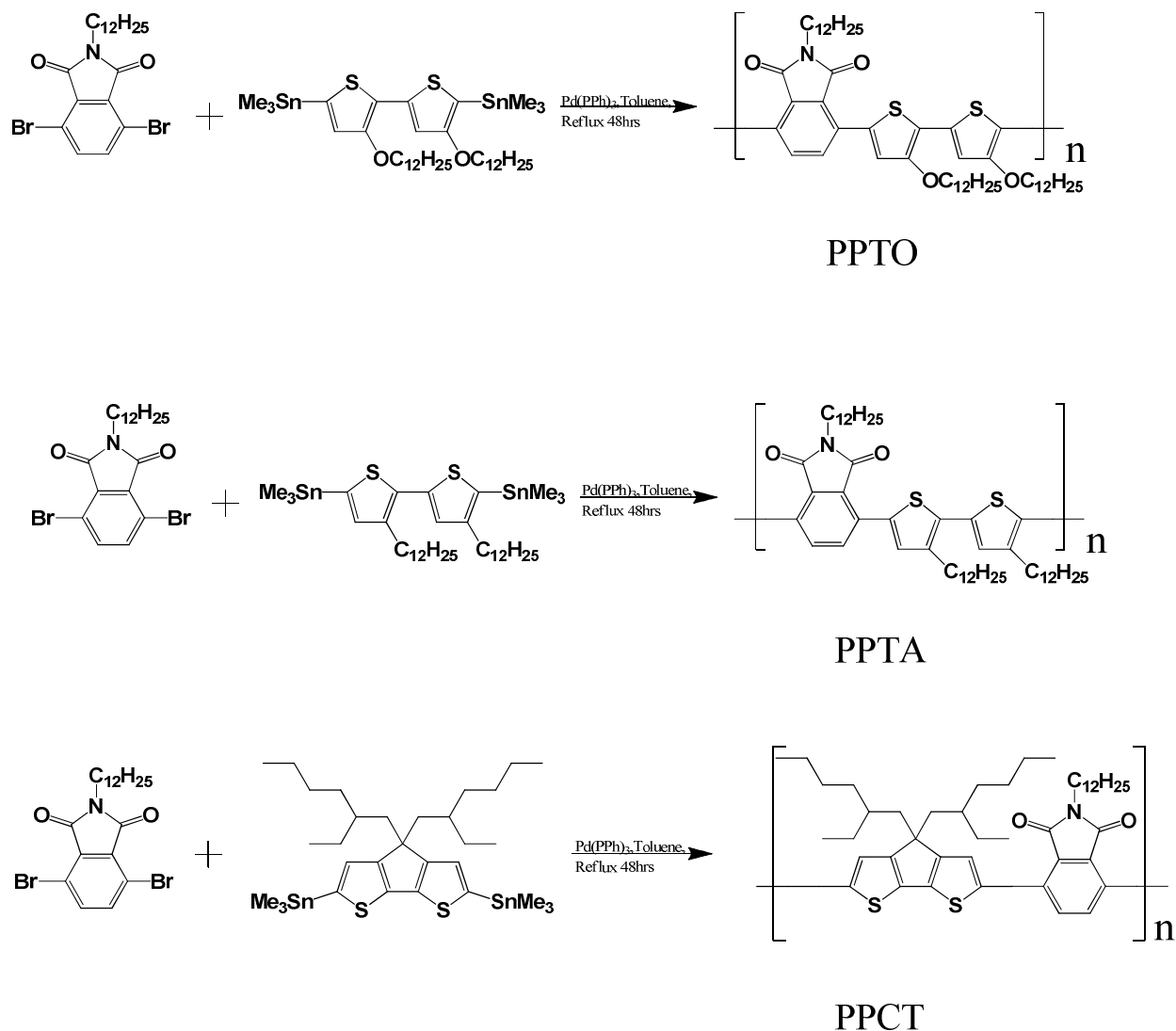Figure 6.1: Carbazole backboned polymers.

Figure 6.2: Phthalimide backboned polymers.

6.3.   Results and Discussion

The UV-VIS absorption spectra of polymers and the corresponding polymer-SWNT complexes were all measured in THF (Figure 6.3). PPTO, PPTA, PPCA, and PPCO-SWNT hybrids absorption peaks that belong to individually dispersed nanotubes. PPC and PPCT do not disperse nanotubes at all. The assigned nanotube chiral indices are given in Figure 6.4. In overall, all polymers disperse similar nanotubes without any chiral selectivity.

55

Table 6.1: GPC Data of Polymers.

Polymer	Mw (g/mol)	Mn (g/mol)	PDI
PPC	6482	3601	1.8
PPCO	4024	3353	1.2
PPTO	6048	4281	1.41
PPCT	20380	15100	1.35
PPTA	3821	2278	1.67
PPCA	4514	1732	2.60

PPTO, PPCO, PPCA, and PPTA exhibit strong emission in solution. Highly efficient quenching of fluorescence occurs when the polymers are adsorbed on the SWNT surface. Figures 5-8 show the 2D excitation-emission map of polymer-SWNT hybrids recorded in THF solution. The chiralities predicted in these maps usually agree with those on absorption spectra. Families of 20 and 21 have been successfully dispersed with phthalimide containing polymers. PPCO has the least solubilizing power and nanotube emission peaks are not clearly observed in excitation-emission map. This is partly due to the strong emission observed from PPCO, which dominates the emission spectra. Raman spectroscopy was further used to identify oligomer-SWNT samples. The sample was prepared by drop casting dilute oligomer-SWNT solution in THF on the microscope glass and then air drying the sample. Raman measurements were performed in air, using an excitation wavelength of 785 nm. The RBM mode peaks are shown in Figure 6.9. The Raman spectra results indicate that each oligomer disperses similar nanotubes, but to a different extent for each chirality. Nonetheless, the mechanism of dispersion and the dependence of solubilizing power on structural features of dispersants are not clear at this moment.
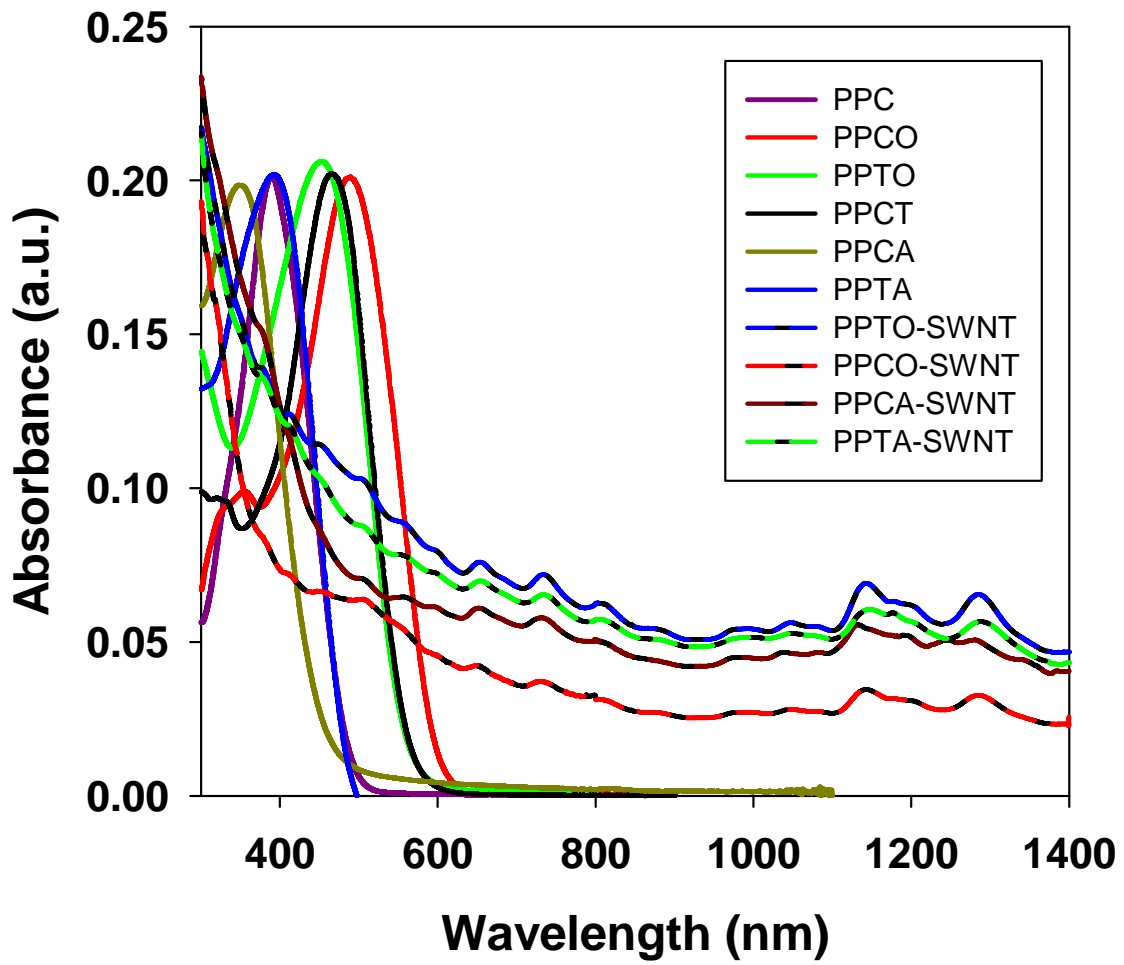
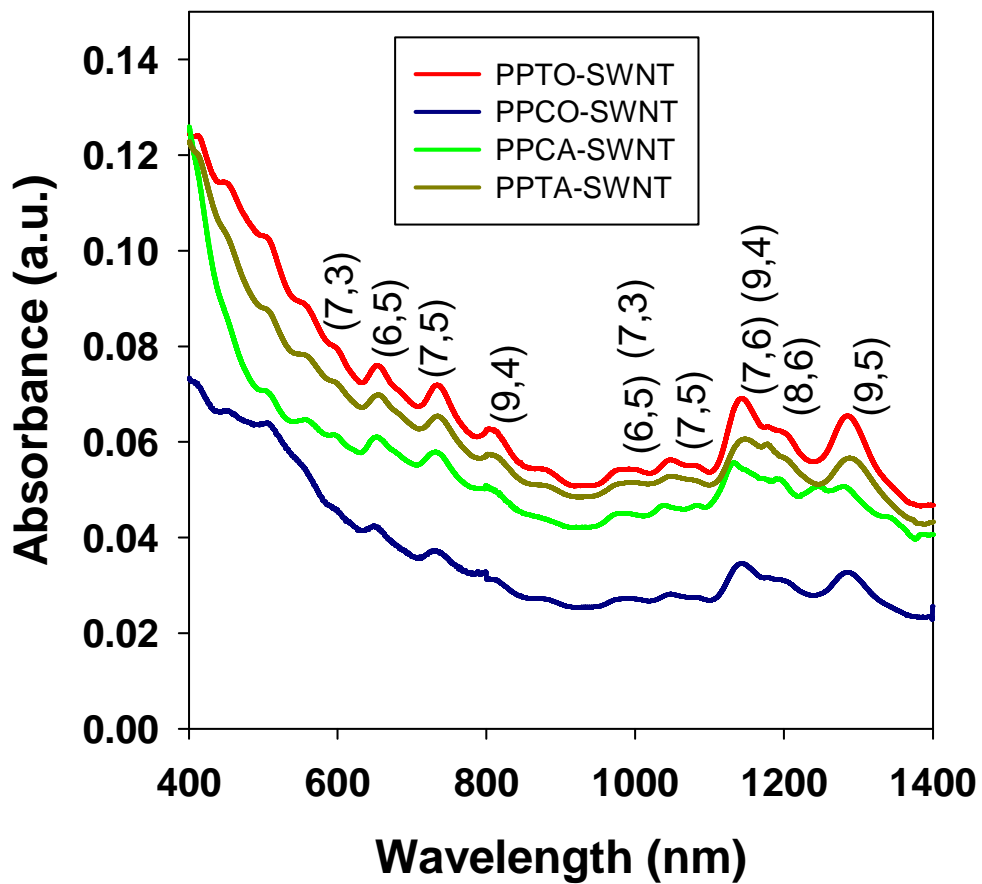Figure 6.3: UV-Vis absorption profiles of polymers and polymer-SWNT hybrids.

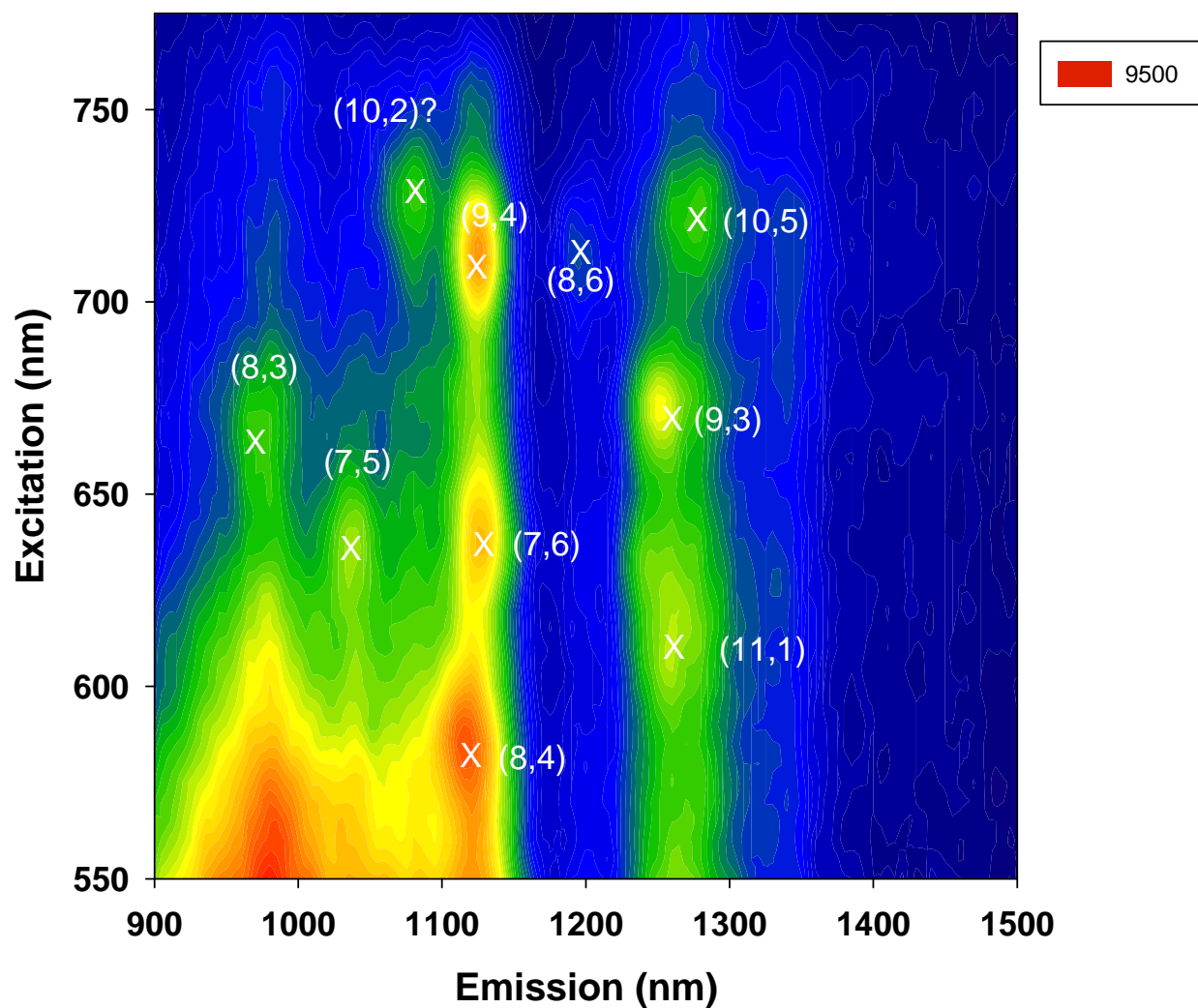Figure 6.4: UV-VIS absorption spectra of polymer-SWNT complexes in THF.

Figure 6.5: 2D excitation-emission map obtained for PPCA-SWNT hybrid.
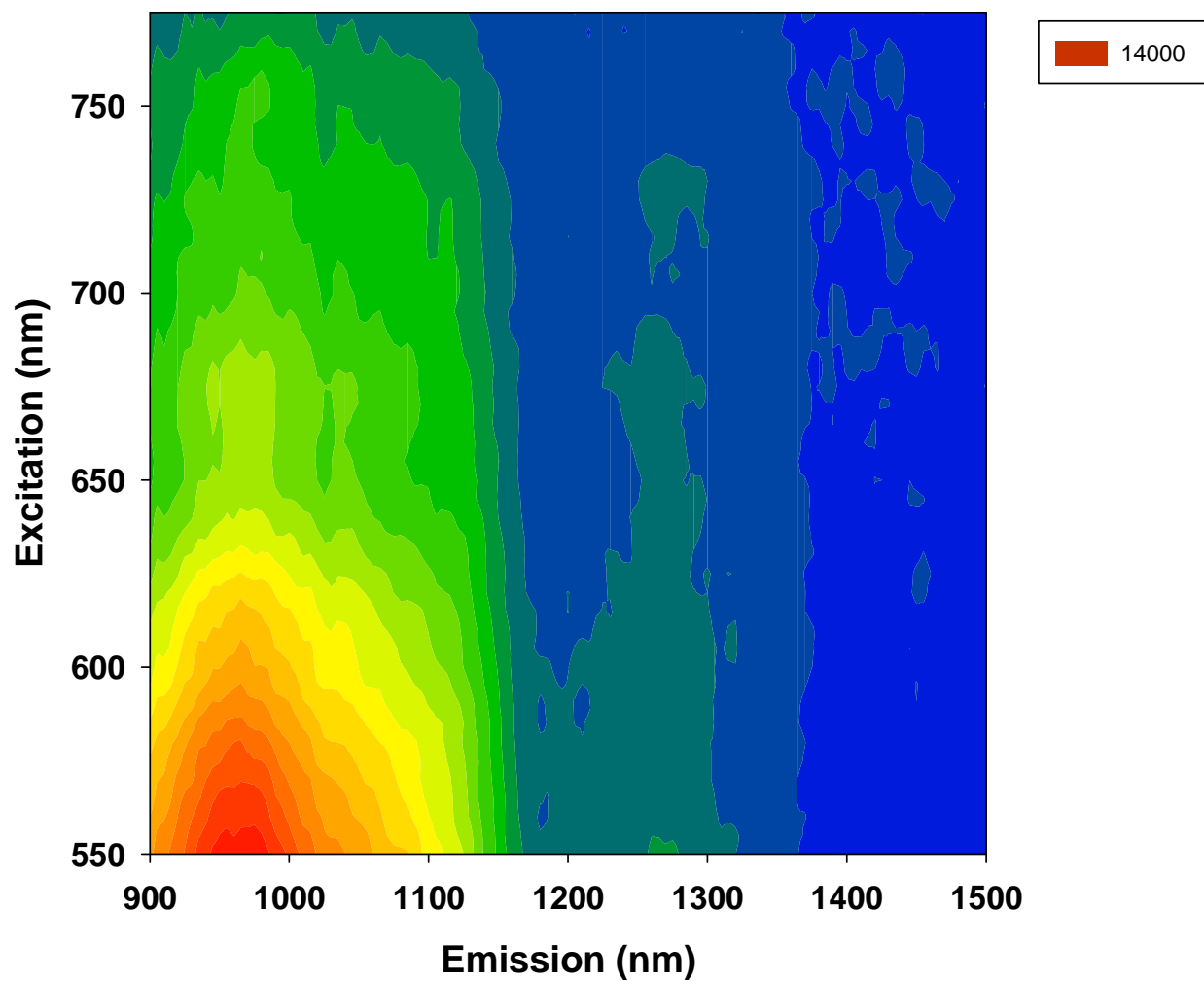
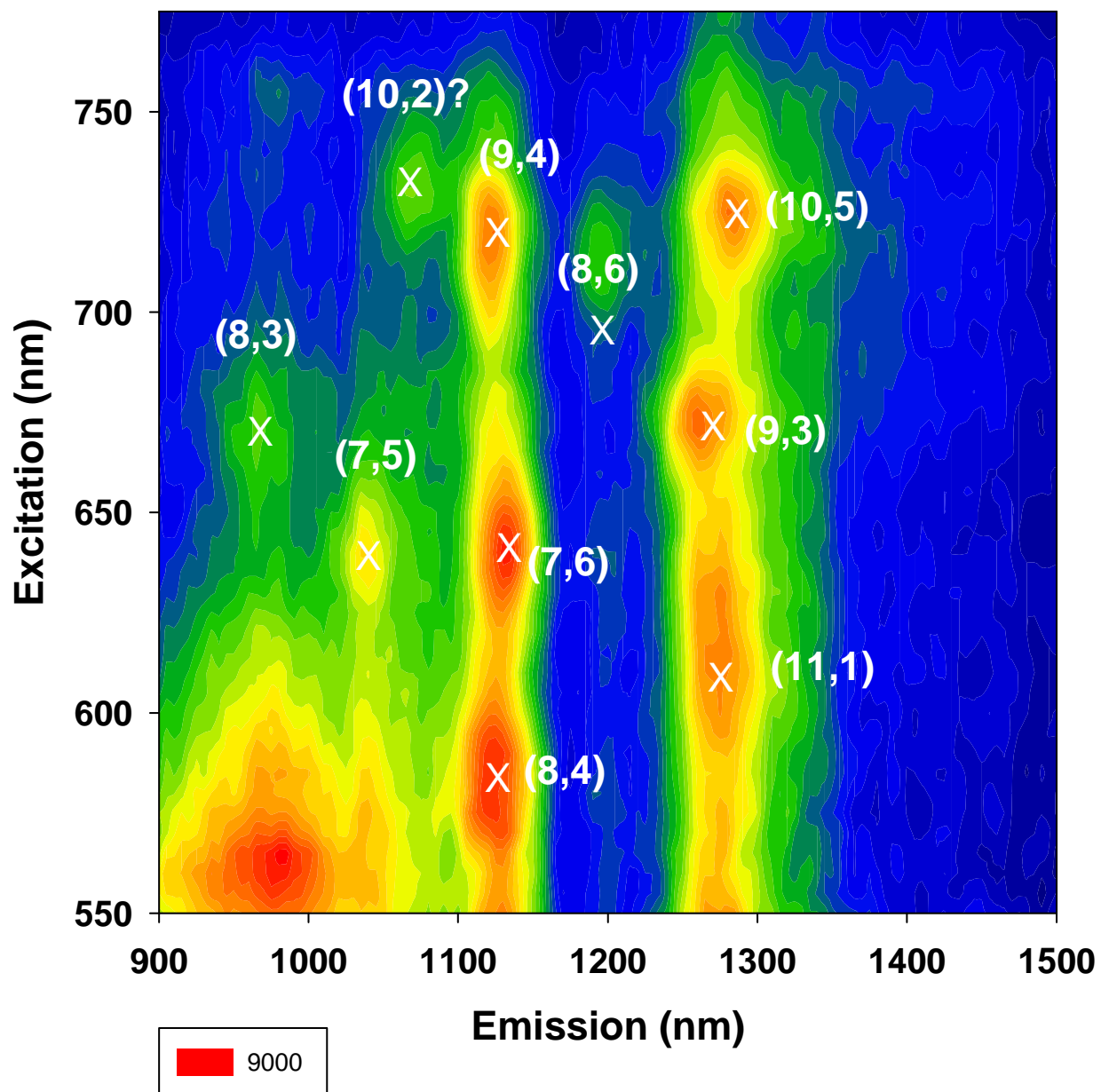Figure 6.6: 2D excitation-emission map obtained for PPCO-SWNT hybrid.

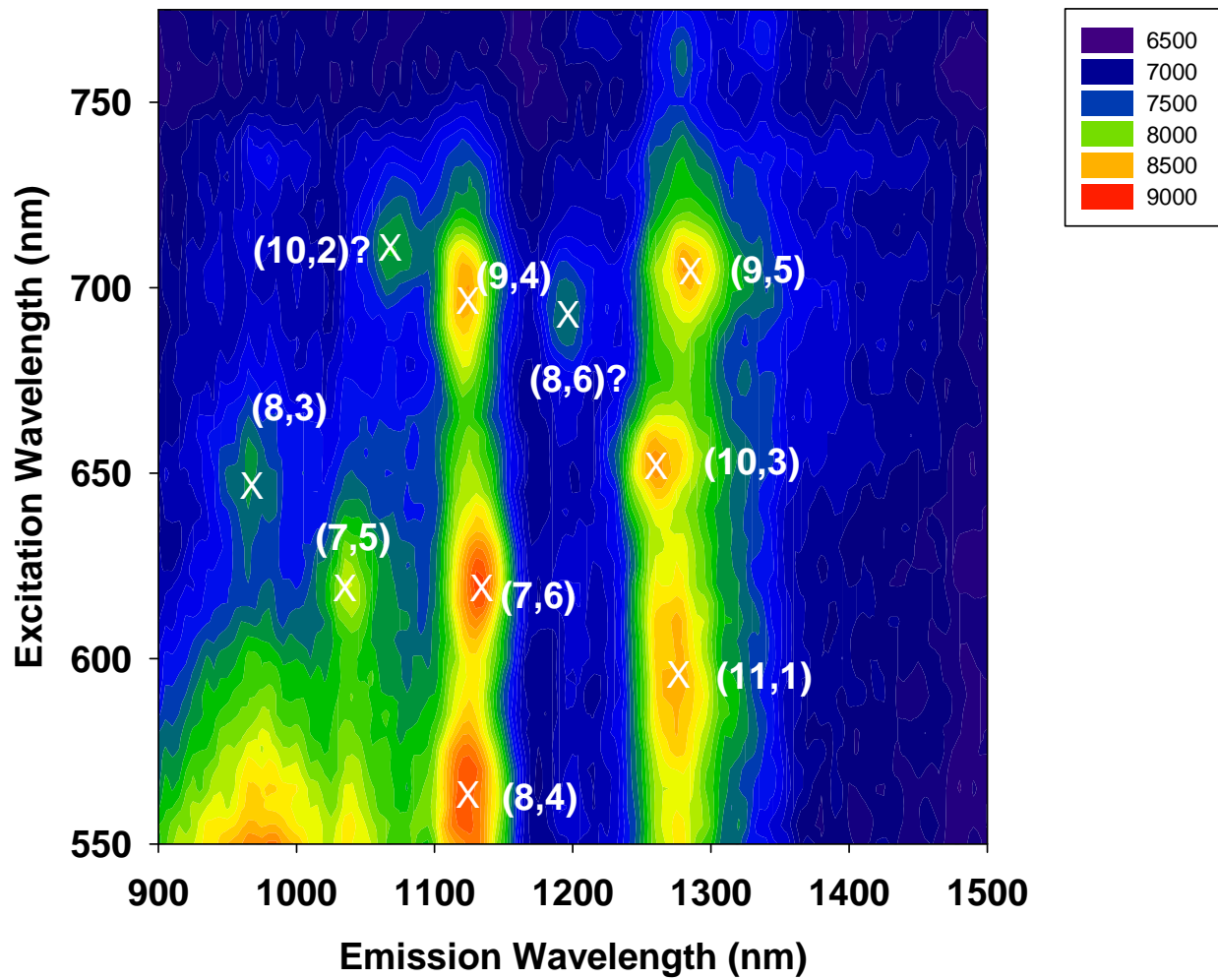Figure 6.7: 2D excitation-emission map obtained for PPTA-SWNT hybrid.

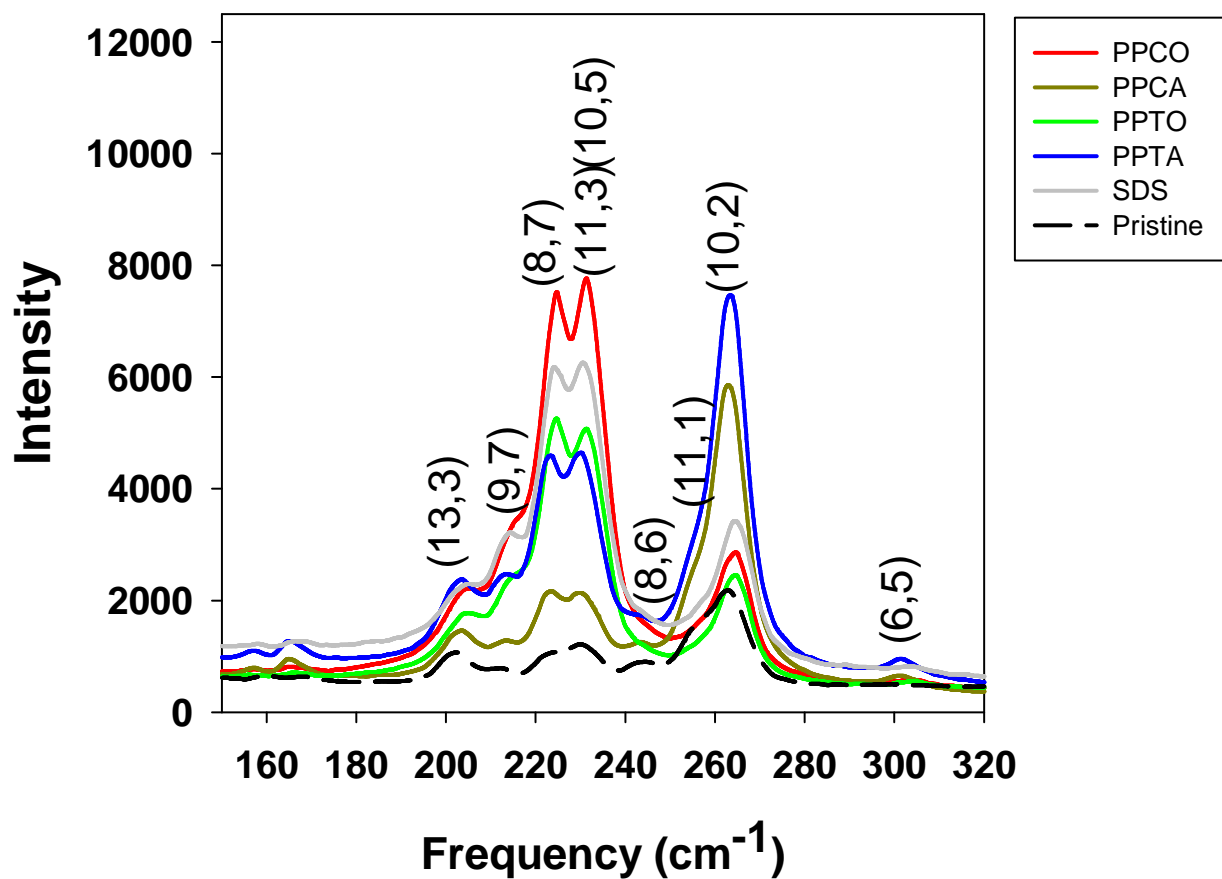Figure 6.8: 2D excitation-emission map obtained for PPTO-SWNT hybrid.

Figure 6.9: Raman spectra of SWNT samples recorded for 785 nm laser excitation.

6.4. Conclusions

We have successfully sensitized phthalimide based polymers and oligomers. Some of these polymers showed high solubilizing power for SWNTs. Though, they all disperse similar nanotubes with little preference to some chiralities. There are major differences in the amount of dispersion capabilities exhibited by these dispersants. Yet, more research is needed to understand the mechanism of dispersion and how polymer structure affects the solubilizing power of these polymers.

6.5. References

1.   Iijima, S. Nature 1991, 354, 56–58.

2.   Ajayan, P. M.; Tour, J. M. Nature 2007, 447, 1066–1068.

3.   Zhang, D. H.; Ryu, K.; Liu, X. L.; Polikarpov, E.; Ly, J.; Tompson, M. E.; Zhou, C. W. Nano Lett. 2006, 6, 1880–1886.

4.   Wu, Z. C.; Chen, Z. H.; Du, X.; Logan, J. M.; Sippel, J.; Nikolou, M.; Kamaras, K.; Reynolds, J. R.; Tanner, D. B.; Hebard, A. F.; Rinzler, A. G. *Science* 2004, 305, 1273–1276.

5.   (a) Nakashima, N.; Tomonari, Y.; Murakami, H. *Chem. Lett.* **2002**, *31*, 638-639. (b) Petrov, P.; Stassin, F.; Pagnoulle, C.; Jerome, R. *Chem. Comm.* **2003**, 2904-2905. (c) Liu, L.; Wang, T.; Li, J.; Guo, Z.-X.; Dai, L.; Zhang, D.; Zhu, D. *Chem. Phys. Lett.* **2003**, *367*, 747-752.

6.   Zhang, J.; Lee, J.-K.; Wu, Y.; Murray, R. W. *Nano Lett.* **2003**, *3*, 403-407.

7.   (a) Zhao, J.; Lu, J. P.; Han, J.; Yang, C.-K. *Appl. Phys. Lett.* **2003**, *82*, 3746-3748. (b) Star, A.; Han, T.-R.; Gabriel, J.-C. P.; Bradley, K.; Gruner, G. *Nano Lett.* **2003**, *3*, 1421-1423.

8.   Murakami, H.; Nomura, T.; Nakashima, N. *Chem. Phys. Lett.* **2003**, *378*, 481-485.

9. Li, H.; Zhou, B.; Lin, Y.; Gu, L.; Wang, W.; Fernando, K. A. S.; Kumar, S.; Allard, L. F.; Sun, Y.-P. *J. Am. Chem. Soc.* **2004**, *126*, 1014-1015.

10. Qu, L. W.; Lin, Y.; Hill, D. E.; Zhou, B.; Wang, W.; Sun, X.; Kitaygorodskiy, A.; Suarez, M.; Connell, J. W.; Allard, L. F.; Sun, Y.-P. *Macromol.* **2004**, *37*, 6055-6060.

11. Fernando, K. A. S.; Lin, Y.; Wang, W.; Kumar, S.; Zhou, B.; Xie, S.-Y.; Cureton, L. T.; Sun, Y.-P. *J. Am. Chem. Soc.* **2004**, *126*, 10234-10235.

12. Pimenta, M. A.; Marucci, A.; Empedocles, S. A.; Bawendi, M. G.; Hanlon, E. B.; Rao, A. M.; Eklund, P. C.; Smalley, R. E.; Dresselhaus, G.; Dresselhaus, M. S. *Phys. Rev. B* **1998**, *58*, R16016-R16019.

13. Ikeda, A.; Nobusawa, K.; Hamano, T.; Kikuchi, J. *Org. Lett.* **2006**, *8*, 5489-5492.

14. B. Kitiyanan *et al.*, *Chem. Phys. Lett*. **317**, 497 (2000).

15. S. M.Bachilo *et al.*, *J.Am. Chem. Soc*. **125**, 11 186 (2003).

16. V. Perebeinos *et al.*, *Phys. Rev. Lett*. **94**, 027402 (2005).

17. F. Plentz *et al.*, *Phys. Rev. Lett*. **95**, 247401 (2005).

18. Y. Miyauchi and S. Maruyama, *Phys. Rev. B* **74**, 035415(2006).

19. Weisman, R. B.; Bachilo, S. M. *Nano Lett*. 2003, 3, 1235–1238.

20. Lebedkin, S.; Hennrich, F.; Kiowski, O.; Kappes, M. M. *Phys. Rev. B* 2008, 77, 165429.

21. Tsyboulski, D.; Rocha, J.-D. R.; Bachilo, S. M.; Cognet, L.; Weisman, R. B. *Nano Lett.* 2007, 7, 3080–3085

22 US Patent 2013/0035464A1

23. Qian, G., Chem. Family of Diazapentalene Chromophores and Narrow-Band-Gap Polymers: Synthesis, Halochromism, Halofluorism, and Visible−Near Infrared Photodetectivity Mater. **2012**, *24*, 2364–2372

24.   Song, S., S. Park, *Synt. Met.*, 2012, **162**(21-22): 1936-1943.

25.   Guo X., J. Am. Chem. Soc. **2009**, *131*, 7206–7207

26.   US Patent WO 2010/079064 A2

27.   By Lee, Jae Min; Baek, Seon Hui; Lim, Jong Seon; Yoon, Seong Cheol; Kim, Dong Uk;

      Lee, Chang Jin From Repub. Korean Kongkae Taeho

      Kongbo (2010), KR 2010086197 A 20100730

28.   US Patent US 2010/0252112

CHAPTER 7. SUMMARY

The purposes of this work are to evaluate the SWNT dispersion capability of a non-planar polyaromatic hydrocarbon derivative and conjugated oligomers and also to establish an effective dispersion method for SWNTs. Motivated by the high solubility of the SWNTs with planar aromatic systems and conjugated materials reported in the literature, a systematic study of the solubility of purified HiPco SWNTs with synthesized dispersants was given in Chapters 5 and 6. Stable dispersions of SWNTs have been demonstrated with PEGylated corannulene compound and phthalimide containing conjugated oligomers/polymers.

UV-vis-NIR, PL, and Raman spectroscopy techniques were used in identification nanotube chiral indices as well as the extent of solubilization achieved by each dispersant. PEGC has been found to disperse SWNTs as effective as commonly used surfactant SDS. PEGC has also tendency to disperse more metallic nanotubes than SDS counterpart. Phthalimide containing oligomers have huge potential in solubilizing nanotubes in common organic solvents. The preliminary experiments indicate various parameters might play significant role in the solubilizing power for each oligomer, which further warrants more studies to be performed on these dispersants.